# External PPG by external pressure on human skin feasibility study

## producing PPG signals on human skin using external air pressure

Shakarchi, H.J.

*Award date:*
2018

**Philips research**, **Eindhoven**

# External PPG by external pressure on human skin feasibility study

January 19

2017

Producing PPG signals on human skin using external air pressure.

**Eindhoven University of Technology (TU/e)**

Student name: Haider Shakarchi

Student number: 0862398

# Contents

# External PPG by external pressure on human skin using air pressure

### *TECHNICAL FIELD*

Measure tissue oxygenation remotely (rStO2), using micro-modulation[1] induced locally on human skin.

### *Glossary*

**cPPG** is the cardiac photoplethysmogram (PPG).
**ePPG** the external PPG induced by air using the micro-modulation.
**DC** is the base-level of the signal.
**raw(n)** the raw signal at sample 'n'.
**$^{n}$PPG(n)** is the normalized signal by 'raw(n)/DC-1' for sample 'n'.
**THM** Traube-Hering-Mayer waves.

## Introduction

Measurement of peripheral arterial oxygen saturation (SpO2) is a widespread practice in many clinical situations. This is because its measurement is non-invasive, relatively easy and provides an indication of the cardio-pulmonary status of an individual.

However, in recent years there has been an increasing interest in measuring hemoglobin oxygen saturation in tissues (%StO2). This is because StO2 directly expresses the microcirculation of tissues which can be used to diagnose ischemia and sepsis at earlier stages [1, 2]. Ischemia is a common disorder characterized by shortness of oxygen supply at tissue level.

As well, through StO2 measurement it is possible to locally determine the status of an organ as the hemoglobin oxygen saturation in tissues can vary depending on the physical structure and status of the tissue, while the SpO2 is a systemic parameter fairly constant everywhere in the body.

A preliminary work was undertaken on measuring StO2 in [3] using the dynamic ratio of oxygenated hemoglobin in the microcirculation to total hemoglobin within an individual at specific place in contact mode. This ratio was measured from wavelengths[2] that penetrate the skin and soft tissues in which some are absorbed by blood chromophores that have specific absorption wavelengths at the different spectrogram regions. Light that is not absorbed is returned as an optical signal and analyzed to produce a ratio of oxygenated hemoglobin to total hemoglobin, expressed as % StO2.

---

[1] Micro-modulation is a controlled modulation by externally induced pressure on skin e.g. by air.

[2] Wavelengths are often in the range of near-infrared region between 700nm and 1000nm known as near-infrared spectroscopy (NIRS).

Although the success of non-invasive contact measurements is useful, there has been an increasing interest in remote measurements as it decreases the risks of infections. Over the past years, a number of researchers have shown that PPG signals can be measured by simple RGB camera in [4] and [5]. In recent years, SpO2 was also measured remotely in [6] and [7] which show that blood oxygen saturation can be measured as well, and in [7] it is demonstrated that it can even be motion robust. Furthermore, in [8] researchers have reported that the camera-based contactless pulse-oximetry is fundamentally feasible. This is because remote SpO2 measurement is not affected by the superficial capillaries contribution. Results showed accuracy of the measurement was significantly lower (<1.65%) than that required by the International Organization for Standardization (ISO) standard. Furthermore in [10], researchers were able to remotely approximate the value of blood oxygenation in tissue (StO2). This was accomplished by using the Spatial Frequency Domain Imaging (SFDI) principle[3]. SFDI measurement characterizes tissue optical properties in time-independent domain. This method is often referred as (DC) method. Alternatively, measuring atrial blood oxygenation (SpO2) is usually done in time-dependent method (i.e., AC) using the cardiac PPG signal.

It is clear in the recent years more attention was focused on remote plethysmographic imaging (rPPG) rather than the widely used contact pulse-oximeters[4]. This is because contact devices may cause discomfort to patients and is impractical in some clinical situations[5]. To date, a number of companies[6] advertise their products for measuring StO2 based on DC-spectroscopy technique. Such products use the SDFI principle to separate the effects of scattering and absorption element to approximate the StO2. However, a major problem with this kind of measurements is that the solutions provided are not always unique. The reflectance of skin spectrum is not unique for a set of skin parameters. In [11], a previous study has indicated the ill-posedness of the visual reflectance spectroscopy and showed how one particular solution may have many alternative reasonable solutions.

Rather than giving an approximation of StO2 and dealing with the uncertainty of solutions, we wondered if it is possible to remotely measure the StO2 in time-dependent method (i.e., AC) to reduce skin parameters and accurately measure the StO2. To date, there has been no study or research which has demonstrated a remote StO2 measurement based on AC method. It is an interesting topic to investigate.

At this stage, the aim of this study is to investigate the feasibility of reproducing PPG signals externally using air pressure. When capillary blood volume varies over time, absorption of light varies too. Consequently, the reflected light is modulated in time domain, similar to the cardiac induced conventional PPG. Such a modulation is then used to measure the StO2 with less complexity (and skin parameters). Using external pressure, a micro-modulation is induced to manipulate capillary blood volume. Such a manipulation will induce changes in light that have traveled and returned from capillary

---

[3] https://scholar.harvard.edu/ndurr/pages/sfdi

[4] Contact pulse-oximeters are devices that are in direct contact with the skin.

[5] At some places skin can be difficult to place measuring probes on, also when the skin is fragile for example by burns or surgery, or in premature infants.

[6] Companies such as Kent Imaging Inc., HyperMed Imaging Inc. and Modulated Imaging Inc.

blood, which can be analyzed to produce the StO2. The oxygenation of blood is then analyzed in AC based method similar to SpO2 measurement. This may lead to accurate StO2 measurement.

## Preliminary knowledge

Measuring SpO2 is often done through the well-known method ratio-of-ratios. This method is quite straight forward and is described in many literatures. In the application report [9], ratio-of-ratios was described and applied using two signals to calculate the SpO2, the signals were red and infrared at 660nm and 900nm respectively. Constants 110 and 25 are the configuration variables. These are often noted as C1 and C2 in literatures. For more information, see figures 1 and 2.

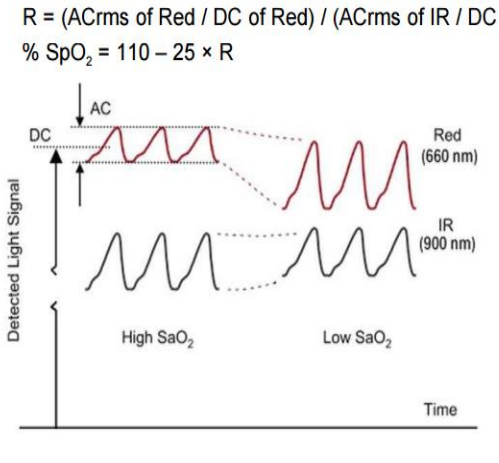


**Figure 1. Red and Infra Red Modulated by Cycling Blood**

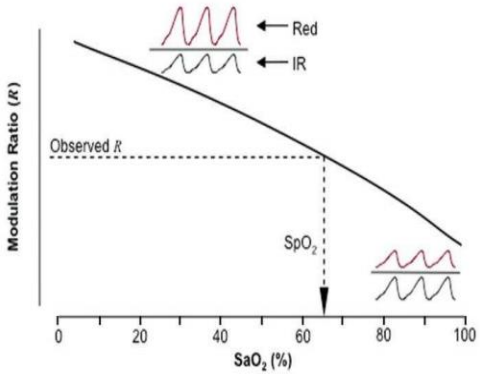


**Figure 2. Red/Infrared Modulation Ratio**

To measure StO2, a similar approach can be used if we can somehow modulate the volume of the blood in capillaries. If external pressures are applied periodically on the skin to empty capillary blood, and then, when the pressure is released blood will flush back to refill the capillaries. Such an emptying and refilling of capillaries will induce changes in light, which may be analyzed to measure the oxygenation of blood. In general, the light returning from vascular tissues often has traveled through different skin layers[7]. By analyzing only relative changes we assume we measure only the skin layer in which we modulated the blood volume: i.e. the superficial dermis with capillary vessels. To mention, overall skin motion at the frequency of modulation may pollute the (optical) measurement, if it results in optical signals. Hence, we required the subjects to remain still while recording. Further the amount of pressure must be quantified to ensure modulation at specific depth, and more importantly, verify reproducibility of the pressure.

In Figure 3 the plot shows the relation of pressure exerted by blood on the walls of a blood vessel. It is worth mentioning that the venules and veins have lower blood pressure than the arterioles. Therefore, we expect the venules and veins to be affected by the micro-modulation before the arterioles. With regards to capillaries, it is not clear yet which one is affected first (capillary or venules). Tissue capillaries are the closest to the skin surface, so it is more likely that the pressure will affect the capillaries first,

[7] Except for blue channel, as blue has less penetration depth.

then the venules and/or veins. Conversely, it is possible to have the venules and/or veins affected before capillaries due to the lack of blood pressure.

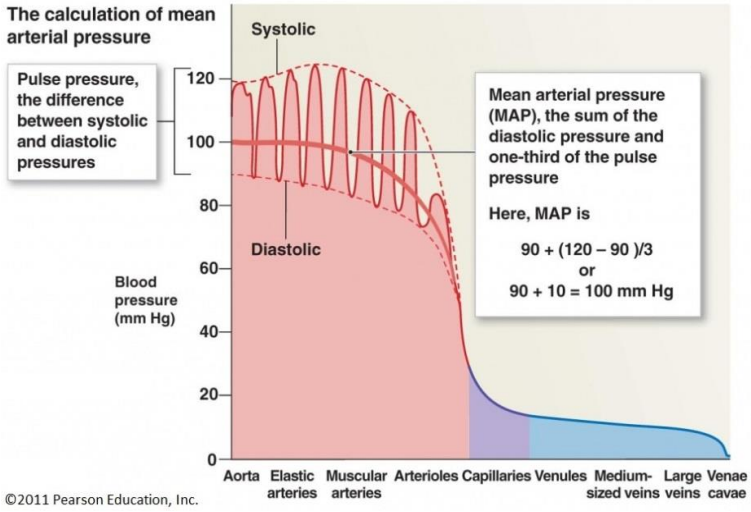


**Figure 3. The hydrostatic pressure exerted by blood on the walls of a blood vessel**

Further, it is important to note that the flow of the blood is regulated for different reasons by various mechanisms. Temperature regulation is one of the reasons to adjust blood flow. When blood vessels constrict, the flow of blood is restricted or decreased to retain body heat. Therefore, during the measurement/experiment temperature change should minimized. In figure 4, the effect of vasoconstriction and vasodilation on blood flow is illustrated.

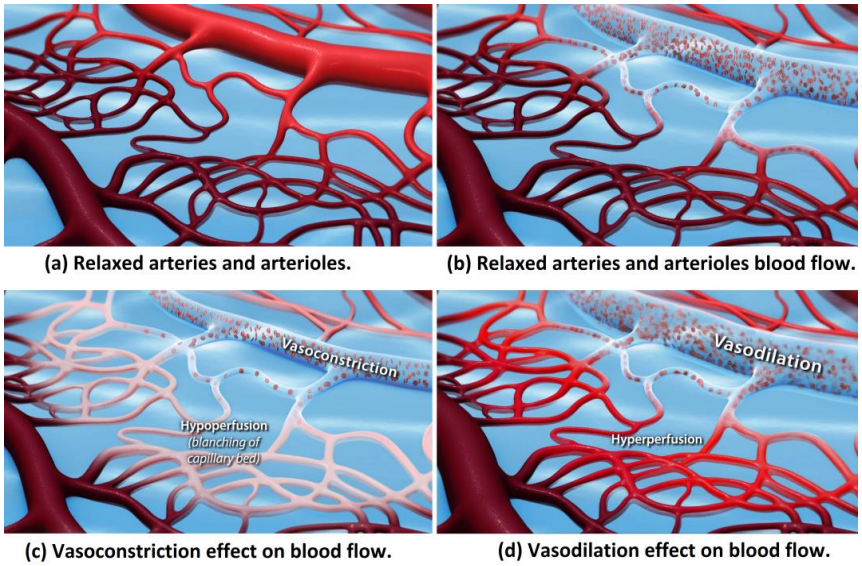


**Figure 4. Blood flow control mechanism to retain body heat or increase vascular resistance (By Joe Samson, The University of Georgia ©2016)**

In addition to vasoconstriction and vasodilation, human body regulates temperature via arteriole-venule shunts (arteriovenous anastomoses). Arteriole-venule shunts are small muscular valves that are directly connected between an arteriole and a venule to bypass the capillaries. In Figure 5, a cross section of skin

diagram showing the multiple layers including blood vessels, arteriovenous anastomoses and capillary beds.

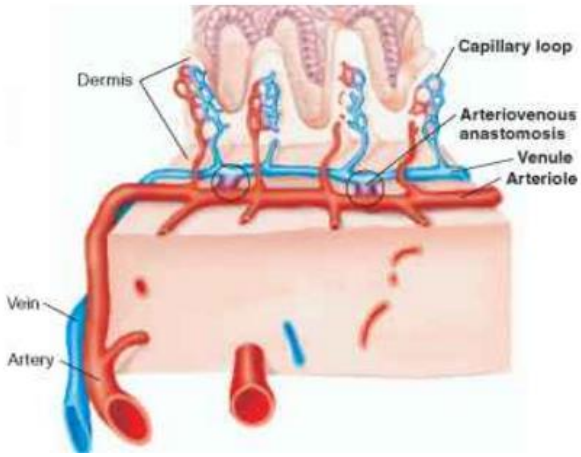


**(https://www.78stepshealth.us/human-physiology/cutaneous-blood-flow.html)**

**Figure 5, Skin cross section**

## Problem Statement

In recent years there has been an increasing interest in measuring StO2. Whereas SpO2 gives a good indication of the functioning of heart and lungs and thus the *supply* of oxygen, the actual uptake of oxygen in an organ is not measured with SpO2. Current solutions for remote StO2 measurements, such as DC reflectance spectroscopy deals with large ranges of values for each skin parameter that satisfactorily fits to a solution. Such an ill-posedness adds some complexity to the system and uncertainty to the provided solutions. In other words, many solutions may fit the measured reflectance spectrum so large uncertainty about the actual values are associated with these methods. Meanwhile, (remote) SpO2 measurement is less complex, accurate, and inexpensive (given that the cardiac PPG signal is measurable). In general, SpO2 measurement depends on the relative amplitude of the cardiac PPG, and it is usually an AC-based measurement (See Figures 1 and 2).

To measure the StO2, a similar approach can be taken as in SpO2 measurement. The light received from the variation of blood volume is measured to analyze the oxygenation saturation in the blood. However, to measure StO2, the cardiac PPG cannot be used, as the cardiac PPG stems from arterioles blood. This is not the appropriate signal to measure StO2. Using the cardiac PPG only arterial blood oxygenation can be measured. The oxygen saturation in tissue can be measured from a place where the oxygen exchange takes place. The exchange of oxygen takes place at the capillaries. Thus to measure StO2, some variation in blood volume at the capillaries must be induced. A comparable PPG signal must be generated from capillary blood. This PPG signal can be induced externally on the skin using air pressure. For simplicity we can call this signal the external PPG (ePPG). To ensure ePPG signal stems from capillary blood the pressure must be comparable to capillary blood pressure. This means that a preliminary work must be done to evaluate pressure parameters such as airflow, nozzle size and distance to skin. Furthermore, applying such a pressure may effects the venules when modulation is applied. Thus it is important to study pressure parameters for some range to get some understanding of the different pressure levels.

Hence, **the main goal of the work presented in this thesis is: to find out if a micro-modulation on the skin can modulate capillary blood (ePPG).**

Then the frequency of modulation, duration of pressure and temperature of the skin will follow at later stages. Such a study is not trivial. Therefore at this stage, this study must be focused mainly on the feasibility and effectiveness of the micro-modulation to produce the ePPG signals. Later work will follow to evaluate the rest of the parameters for this method. Despite those studies, this method may be more accurate and less complex than the current solutions because its AC principle cancels out the impact of many skin parameters that convolute the DC methods, such as scattering, epidermal melanin etcetera.

## Research Objectives

This feasibility study is mainly to answer the following question:

> "Can we demonstrate using micro-modulation external PPG induced on capillary blood?"

However, to apply external pressure comparable to capillary blood pressure, a preliminary work has to be done to evaluate pressure parameters applied on the skin. Such a preliminary work is useful and important since each blood vessel type contains different blood pressure. This will ensure correct and reproducible results. If we will find differential results between subjects or anatomical locations we should be sure it is due to skin-mechanical and physiological causes, not to variation in the pressure applied. So, a good knowledge about the pressure device is important.

Secondly the following questions are addressed in further studies,

1. Can we design micro-modulation geometries/pressure so that we disentangle capillaries and venules?
2. How can we best control the local pressure for micro-modulation?

## Materials and methods for pressure experiments

To quantify the pressure, a number of experiments were conducted in two methods. First we introduce the general idea, then discuss the two methods and evaluate results.

The general idea as shown in figure 6, was to apply air force from nozzle perpendicular to flat probe made from solid carton attached on laboratory scale 'model: PB1502-S/FACT '. The probe is carefully cut into circular shape within specific size and attached via sturdy tube onto the scale. The tube is made from firm robust plastic to minimize the risk of vibration, which may be caused by the air spurt. This will ensure less measurement distortion. Then scale areas exposed to air were isolated to make sure only probe force is measured. The pressure is calculated by the formula "Pressure (g/ $mm^2$) = Force (gram) / Area ($mm^2$)", where the Area is probe area and the Force is the weight measured. To measure the distance between the nozzle and probe a sensor 'model: ST-VL6180X' is used. Both, the scale and sensor are sampled in parallel by a PC, and then results were stored for offline analysis. The airflow is measured by a flowmeter range between 1-25 liters per minute (L/Min) set manually at each experiment. In figure 6, a sketch of the basic setup is given.

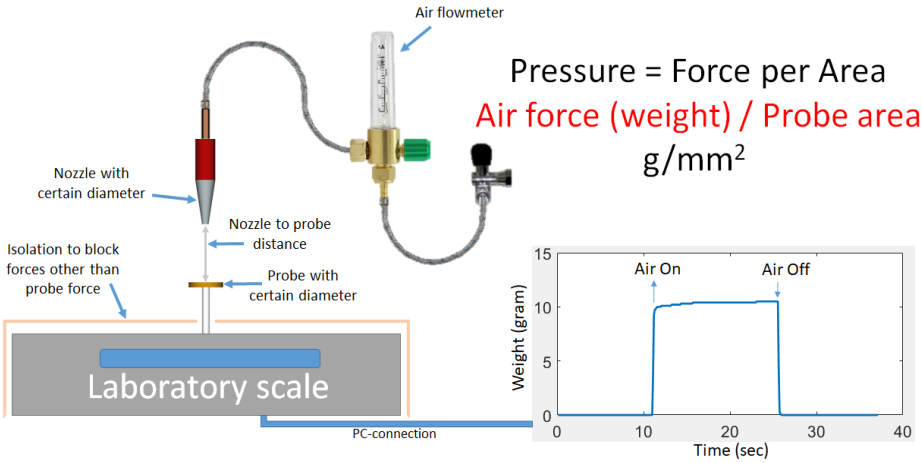


**Figure 6, Basic setup to quantify pressure**

Furthermore, parameters of pressure were defined within reasonable size to keep the number of measurements manageable. We chose 3 nozzle diameters (2.5, 3.5 and 5mm), 5 airflows (5, 10, 15, 20 and 25 L/min) and 6 nozzle-probe distances (10, 20, 30, 40, 50 and 60mm). At a glance during the initial tests, we found that the nozzle with diameter 2.5mm has wider range of pressure. The larger diameter nozzles needed more airflow to keep the pressure in the range of capillary blood pressure. This could cause multiple issues such as rapid decrease in skin temperature, or else, when the airflow is reduced to minimum, the distance to the skin needs to be very close which makes it impractical. Hence, we mainly focused on nozzle with diameter 2.5mm. Other nozzle diameters are studied less intensively. To measure the pressure of air accurately, the probe area should be minimized, as this will ensure that the measured value is close to real pressure. Using larger probes, will results in pressure not equal to center pressure; hence, we used small probe diameters ranging from 4 to 11 millimeters.

### I. Method A: (lateral scan through probe center)

To study the distribution of the air jet on probe area, a second sensor[8] 'model: ST-VL53l0X' was added to register the distance of the nozzle from probe center (register movements in x-direction). Both measurements (the weight and distance) are synchronized such that a profile is obtained for each intersection between the air jet and probe area. The probe was scanned laterally through the jet center in one direction, to get results similar to results shown in figure 7. Despite the linear movement in the x direction, the graph of weight was not symmetrical due to scale/probe hysteresis. However this issue did not affect our measurements, as we are interested in values around the center not the edges.

[8] A fully integrated miniature module measures distance using time-of-Flight (ToF) technology.

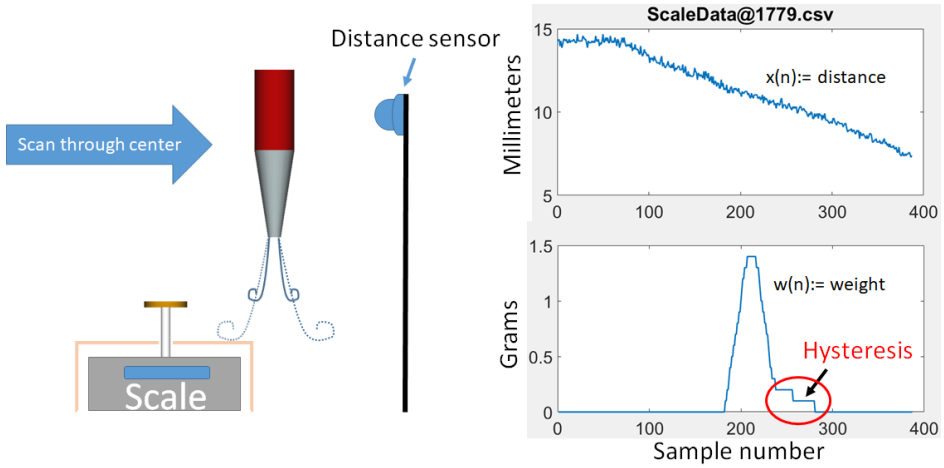


**Figure 7, method A (lateral scan through center)**

Thus, to increase confidence in the results and minimize scale hysteresis, each lateral scan is repeated 6 times (3 times back and forth). Then, sensor noise for both scale and distance are filtered out. Using the probe size, the average pressure was then calculated. Furthermore, to average the 6 measurements, we had to resample and center the distance to the probe center to ensure the 6 measurements are correctly aligned. The average is then calculated using the median over the 6 scans. In graph 1, the final result is plotted for one set of parameters (Nozzle diameter=2.5mm, flow rate=15L/min, Nozzle-probe=20mm).

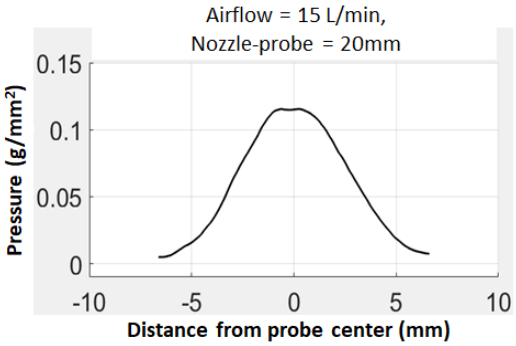


**Graph 1, an scan profile for one parameter set (Airflow,Nozzle)**

Similarly, we processed 5 airflows (5, 10, 15, 20 and 25 L/min) and 6 nozzle-probe distances. The profiles are scanned with the smallest probe so that accurate results are measured. The smallest probe used was 4 millimeters. Due to time constraints we restricted these measurements to the 2.5 millimeters nozzle diameter. In total we obtained 30 profiles which are plotted in Figure 8. Data for distances 30 and 50 millimeters were lower than expected, as they were accidentally measured off-center. As far as capillary blood pressure was concerned, the pressure was comparable for nozzle distances 10 and 20 millimeters. When the results were analyzed we found that the pressure is proportional to flow rate squared. Furthermore, this relation was studied for larger probe sizes, which showed similar results, hence, the relationship was reproducible. However, when the probe diameter was increased, the pressure decreased; this meant the area is larger than the air jet. To investigate the geometry of air jet, we used the results of the smallest probe (4mm) to calculate the Full Width Half Maximum (FWHM) for each profile of the various distances and flow rates. Then, all FWHMs are averaged using median average and

the results of off-center measurements were interpolated. Please note that close to the nozzle, the real FWHM must be less than what we measured because the air jet is most likely smaller than probe diameter (nozzle diameter is 2.5mm < 4mm probe diameter), but it must also be larger than the nozzle diameter. Also note that the shape is likely to change with the distance away from the nozzle. Thus we took best guess line, intersecting with FWHM at distance 0 equal to the nozzle size and at distance 60 millimeter with corresponding FWHM. Then, each probe diameter (4, 7, and 11mm) are classified by corresponding best guess distance. We classified measurements to be reliable when probe diameter is 2 times smaller than the FWHM. This classification showed that even when probe diameter was 4 millimeters it did not accurately represent the real pressure at probe center. Thus to measure the real pressure near probe center accurately, we conceived of a second method which is described next (method B).

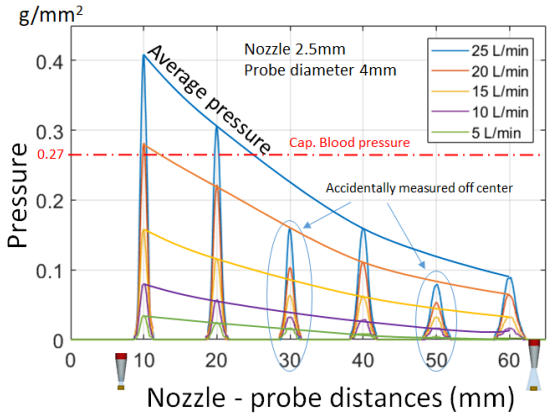


**Figure 8, Pressure results for nozzle 2.5mm for 4mm probe diameter**

### II. Method B: differential method

As the name implies, this approach is based on measuring the difference in force between probe sizes. In this method, we used the same setup to measure various probe sizes from probe center only. The probe diameters range from 4 to 10 millimeters. The values for probe diameters 1, 2 and 3 millimeters were extrapolated using a 2$^{nd}$ order fitting curve. The 2$^{nd}$ order curve was fitted to the data of probe sizes 4-10 millimeters. Furthermore, to ensure smooth flow of pressure distribution, the measured values are interpolated using the fitting curve. Please note that the extrapolation of points must be done for small ranges of values, and the generation of the fitting curve must have very small error. This will ensure correct estimation close to the real values. The absolute error was at most 0.007 (less than 1%) for nozzle distance 20 millimeters. In our case, 30% of the points were extrapolated, which may still miss to estimate the real pressure. Differences of area and weight between two consecutive probe diameters are then calculated. Using the differences of area and weight we calculate the pressure for each difference. We obtained for each difference the average pressure. Since the difference between two consecutive probe diameters is one millimeter, the resolution of obtained profiles was then one millimeter. Furthermore, this method was evaluated by comparing results with method A; results were comparable except for distances shorter than 2 millimeters from center. This was expected since the first method failed to measure values near probe center. In Figure 9, comparison of a profile measured by method A and B are plotted including illustration of method B calculation.

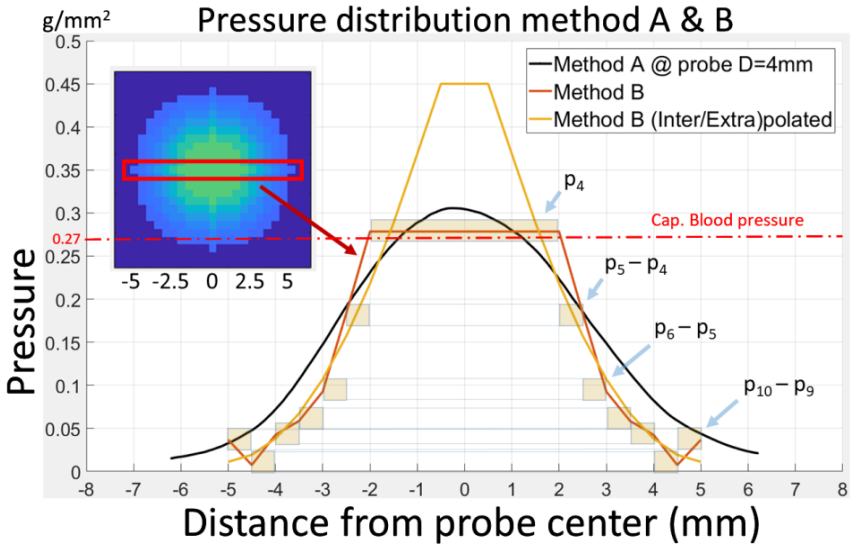


**Figure 9, Comparing Method A and B**

Finally, the various flow rates and distances using method B were then plotted into single graph as shown in Figure 10, results were converted to 'mmHg' units, and parameters set for distance 20 millimeter were chosen for external PPG experiments. This set had the most comparable pressure to capillary blood pressure.

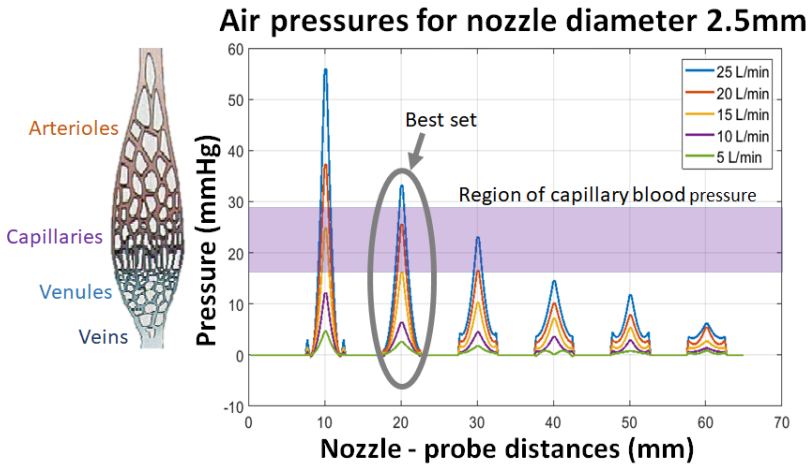


**Figure 10, Pressure results by Method B**

## Materials and methods for external PPG experiments

To measure PPG signals remotely, we used microprobe-lens 'model: Volpi AS 14/50'. This microprobe has C-mount connection which can be used for various sensors. The nozzle of air (with diameter 2.5 millimeter) is firmly attached close to the lens of microprobe. Then, both units are mounted tightly on a rigid stand so that noise from vibration is minimized. Furthermore, a control unit was designed to measure the cardiac PPG from a contact pulse sensor 'model: SEN-11574' and control switching activity of the air and light source using commands received from a PC. Additionally, a second controller was

added to read data from distance sensor 'model: ST-VL6180X' attached at nozzle level to measure the distance between the nozzle and skin. The communication between the PC and both controllers was via RS-232 protocol at baud rate 112500Kbs. Using the PC, the signals from the remote PPG sensor and the data from the cardiac PPG are pulled simultaneously in parallel at fixed frame rate ranges between 15-20 frames per second. All data were then stored on the PC for offline analysis. To ensure stable frame rate between acquiring and writing the data, we buffered the data internally during write operations. To ensure correct buffer access, the design pattern 'producer/consumer' was used. Furthermore, the traffic on the serial bus was reduced using short commands. Please note that the operating system used is not a real-time system. Timing of pulling data may still have some jitter between units due to buffering and high CPU usage. This can be caused by updates or programs running in the background or user interface interactions with the software (LabView). To lower the load, we visualized only important data, thus the acquired data used was only from the remote sensor and contact pulse-sensor. Furthermore, we put timestamps for each sample. This will allow us to resample the data if necessary. In the appendix, both micro-controller's firmware and communication commands are documented, including an instruction manual on how to use the software. Furthermore, a DC powered light source was designed specifically to fit the microprobe-lens. The original light source had frequency noise of 60Hz. We designed the light source with powerful halogen lamp '24volts 250 watt' to have enough intensity in case a spectrometer was used. It was powered by a DC laboratory power supply 'model: SM7020-D'. The halogen lamp was chosen since it delivers high intensities and broad spectrum.

To align the microprobe-lens and nozzle to a single point, the camera 'UI-3060CP-C-HQ' was used. Due to space limitations, the angle between both units was approximately 20˚. We placed area of skin (hand) at a distance of 20mm and aligned skin indentation (caused by the air jet) to the image center. The distance between the camera and lens was then adjusted by a 5 millimeter ring to cover only area of air pressure, and then we adjusted the focus using the microprobe-lens focus wheel. Using this approach, we can process the entire image, which is the most suitable solution to all sensors. Furthermore, to ensure a scenario as in pressure experiments (air was perpendicular to probe/skin), we maximized the angle to the most vertical to the skin for both units. We set both units to near perpendicular rather than only the nozzle, due to the limitation of the light source which was fixed around the lens.

To measure PPG signals, different sensors can be used. We chose to use spectrometer 'model: Ocean optics usb2000' since it can measure in near-infrared and a provide wider range of wavelengths at higher wavelength resolution than a camera. Modern cameras can measure in near-infrared as well, but they offer far fewer channels than a spectrometer. Since this study is in its earlier stages, it may be useful to explore a wide range of wavelengths to target which wavelengths has the most reproducible results for ePPG, as this may be helpful for future studies. We first want to verify that our 'PPG' signals are indeed related to blood volume changes, which is easier when full spectral information is available.

During initial tests, we found that the distance sensor fails to measure the distance while the light source was on. The light source was powerful such that signal of (ToF) from the sensor is distorted. Hence, in each experiment we measured the distance first then we conducted the experiment. In addition, we found that the measured signals were too noisy. To reduce the noise level, we used a longer analysis window, as consequence of long measurement duration. It was very challenging to keep the subject calm, quiet, and without motion for long periods. Furthermore, we found that the cardiac PPG is much weaker than the external PPG (with the air pressures used at least). At this stage we did not estimate this difference since the cardiac PPG strength is location dependent. Furthermore, we found

that the signal of the external PPG is the opposite of the cardiac PPG. When the air pressure is applied on the skin, it will temporarily reduce the blood volume, while the cardiac PPG is caused by temporary increase in blood volume.

Furthermore, since this setup might be used in future studies, we have developed two software versions, one for spectrometer and one for the camera. Both versions acquire data in a similar way, except some extra features were added to the camera version. Using the camera, variations of images in time domain are calculated using the standard-deviation, then shown in real-time. This feature might be helpful to show areas of variations while measuring. The software operates in two modes, one with fixed modulation frequency and the other uses a profile to apply multiple sequences of modulation. To use the profiled mode, the sequences of modulation must be set in advance. The profile is set by duration, frequency, duty-cycle and state of light (1=on/0=off). We used mostly the profiled mode, since it allows us to acquire multiple measurements from the same spot. This was useful to measure cPPG first, and then in the next sequence measuring the ePPG or vice versa.

Different skin sites were measured, but both cPPG and ePPG signals were measured from the same spot. This allowed us to compare blood oxygenation between both PPG spectra. This was done for locations containing strong cardiac PPG signals such as the thenar eminence, hypothenar eminence, back of the hand, the center of hand palm, and also for location containing weak cardiac PPG signals such as the lower arm. The skin was modulated in frequency ranges between 0.1 and 0.4 Hertz. Please note that the range of modulation may have some interference with Traube-Hering-Mayer (THM) waves and respiratory rate. This may also interfere with the cardiac PPG for sites containing strong signals. In Figure 11, on the left, the raw signals recorded by the system are plotted, and on the right only wavelengths 577,670 and 805mn are plotted including the air state and PPG sensor.

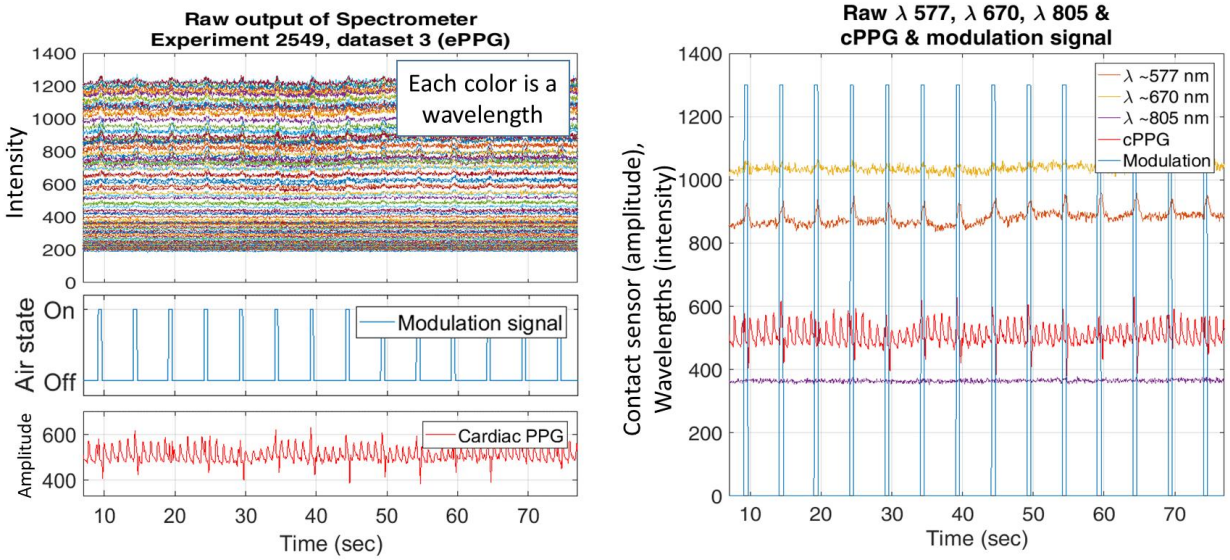


**Figure 11, on the left, all experiment signals (spectrometer, air state and contact PPG sensor) and on the right a plot for only wavelengths 577,670 and 805 including air state and PPG sensor**

To ensure correct measurements, we subtracted the dark[9] current offset from each channel. The offset was measured from wavelengths that have no intensity from light. Furthermore, we calculated the reflectance of the skin which shown in Figure 12 (at the right). We measured the spectrum of light from white paper (A4) at 20 millimeters distance. Similarly, this was done for the skin while the subject remained still. Then, for each signal the median was calculated. This result is often referred to as DC spectrum. To ensure correct results, the duration of both measurements was one-minute long. To make the skin result independent of light reflectance, we divide the DC spectrum of the skin by the DC spectrum of paper. This division is element wise division, per signals median. In Figure 12, at the left both DC spectra are shown and at the right the skin reflectance. The skin reflectance was as expected except for some, they were very noisy. The light source did not cover all wavelengths, but for wavelengths between 450 to 800 nanometers results were stable. Please note that the noise of the short wavelengths was due to minimum light, while for the long wavelengths was due to the sensor sensitivity of the silicon.

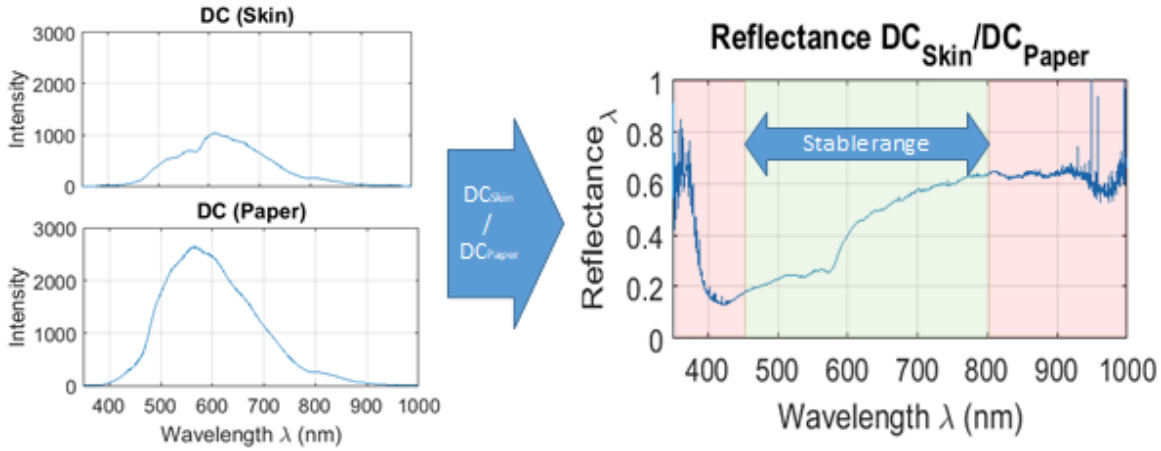


**Figure 12, on the left, the DC spectra for white paper and hand and on the right skin reflectance**

To process the data, we first resampled the data to exact frame rate using the time stamps of samples, and then select clean measurements to analyze.

To calculate the DC level accurately, we chose to process only instances while the modulation from the air jet is off. This was done for each channel individually. The DC was defined by the following formula: '$DC_\lambda = median( raw_\lambda (n) )$' where the $Raw_\lambda(n)$ is the raw value of sample 'n' measured from channel (λ). Please note that this was applied only for samples with the modulation off, and other samples skipped. As in normal PPG, we normalized the signals: '$nPPG_\lambda(n) = [raw_\lambda (n)/DC_\lambda] -1$'. This was done for each of the 2048 wavelength channels (ranging between 350 and 1022 nanometers). To calculate the spectrum of the induced PPG signal (the ePPG spectrum), we transformed the data into frequency domain using the Fast Fourier transform (FFT). For each channel we plotted the fundamental sinusoid obtained by the 'FFT' for frequency equal to the frequency of modulation. In Figure 13, this process is shown for three wavelengths.

[9] The dark current offset is the intensity offset caused by the sensor while the intensity of light is zero.

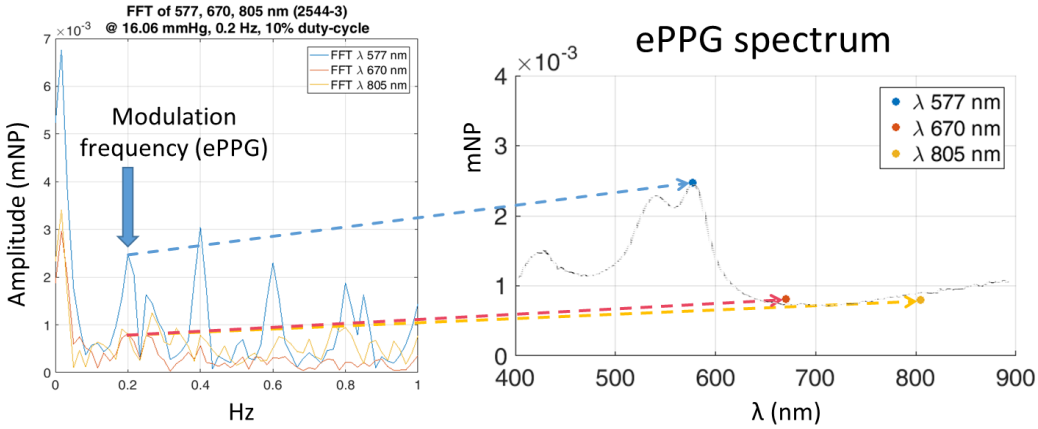


**Figure 13, FFT on left and on right ePPG specturm by FFT for three wavelengths**

However, the shape of the ePPG spectrum was not as expected. There were discontinuities in the red where normally the cPPG signal is very low: a minimum seemed to be inverted to a maximum (figure13). This was confirmed when we analyzed the phase offset of the basic sinusoid of modulation frequency. We found 180 degrees shifts in phase offset for wavelengths between 600 and 750 nanometers. In Figure 14, the resulting spectrum using FFT is on the left, plotted including the expected results and on right the phase offset is plotted for all wavelengths.

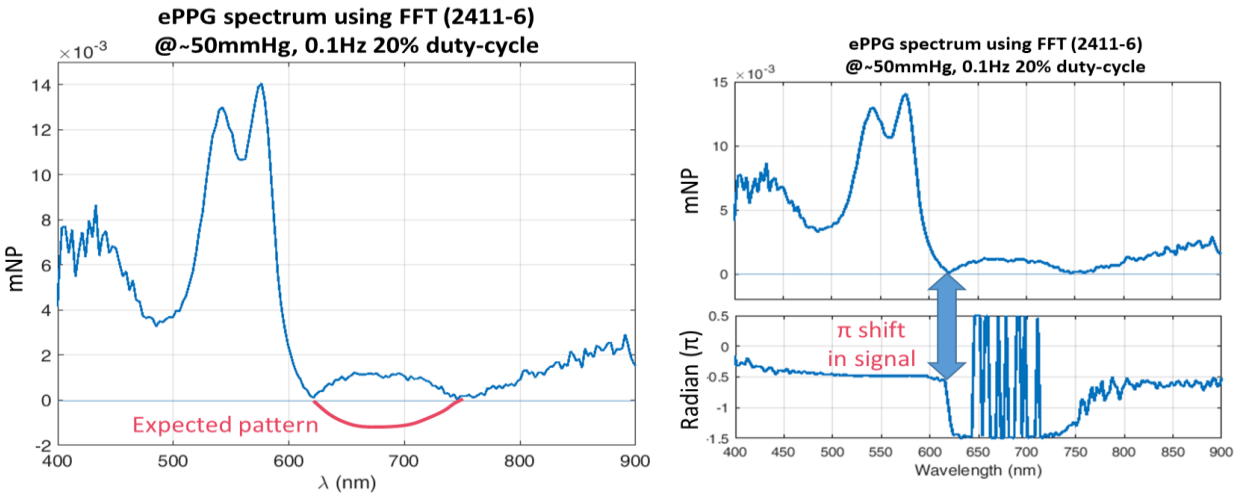


**Figure 14, ePPG spectrum using FFT on the left and on the right at the bottom the phase offset for each wavelength**

When the data were analyzed in time domain, we found that the modulation was affecting the intensity of the reflectance signals. This was our intention of course, but we expected the reflectance intensity to **increase** as we would push away blood (ePPG). Instead, the intensity was **dropping** somewhat during modulation. We quickly found this is due to skin geometry changing during modulation. In Figure 15, an illustration of the geometric effect.

The reduced reflectance intensity caused by the geometry change is constant for all wavelengths, while for the ePPG signal it is not. Consequently, the amplitude of the signal for some wavelengths became negative while for others it became positive. Furthermore, changes in skin geometrics were increasing the distance between skin and air nozzle, which led to decrease in pressure. The distance was estimated to be less than 3 millimeters, which at most may decrease the pressure by 9 %. Despite the decrease in pressure, the pressure was still within the range of capillary blood pressure.

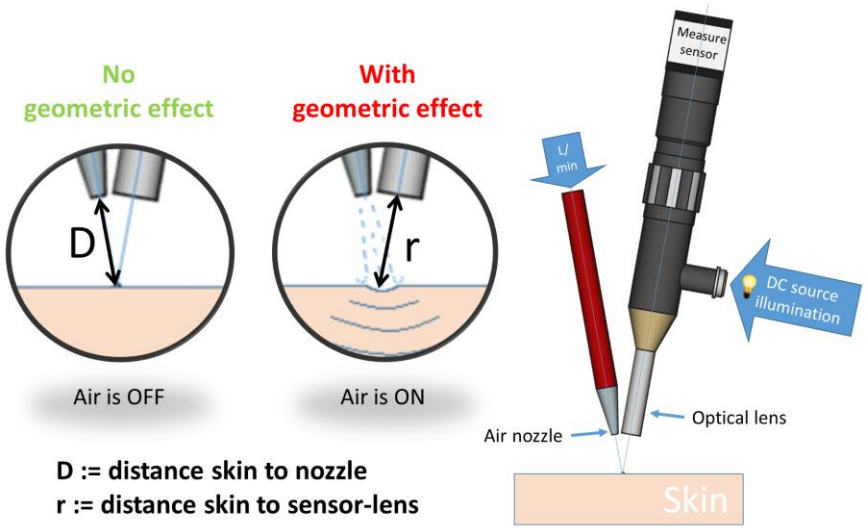


**Figure 15, an illustration of geometric effect**

Furthermore, the pressure was lowered to minimize the geometric effect, but this did not satisfactorily solve the issue. When the pressure was lowered, it was smaller than from capillary blood pressure, and sensor noise started to dominate the PPG signal, especially for wavelengths between 600 and 900 nanometers.

Even though the issue of skin geometry changes is not desired for our purpose, we suggest studying this issue in future studies since it may lead to skin elasticity or firmness measurement. This issue can be solved using a more homogenous (diffuse illumination from all angles) light source to keep the intensity equal even when geometric effects are occurring. Or, perhaps using a protocol to measure first the geometric effect, and then compensate for the relative change. For now, we focused on spectrum shape to evaluate the ePPG blood oxygenation. By comparing the spectrum of the cardiac PPG and external PPG, difference can still be found in blood oxygenation, without having the need for calibration. To calculate the spectrum for negative and positive values, we used the 'dot' and 'segmented' method. Below both methods are discussed.

### I. Method A: dot operation

The intention of this method is to estimate signal amplitude for negative and positive values. It assumes known signal-phase and frequency. The frequency is modulation frequency and the phase can be calculated using the FFT for wavelength of 577 nanometers at frequency of modulation. To construct the ePPG spectrum, we restricted the data to only complete cycles using the knowledge of modulation start and frequency. This will allow us to calculate the correct phase using the FFT. All wavelengths were then normalized as described earlier. Using the FFT analysis, the phase of modulation frequency was calculated from wavelength of 577 nanometers. Using the phase and frequency, we generated a sine

wave with 'sin (π/2–phase)'. This will ensure the sine wave is aligned with the signal. For each wavelength, the dot product of the sine wave and signal was calculated. Next, each result is divided by the number of samples. In Figure 16, result of ePPG spectrum with geometric effect using dot and FFT method is illustrated.

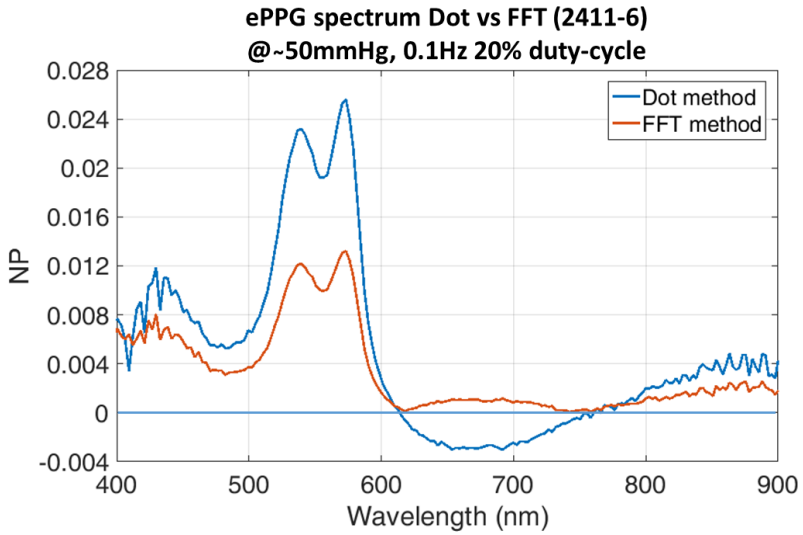


**Figure 16, Result of ePPG spectrum with geometric effect using dot and FFT method**

As can be seen from Figure 16, the shape of the spectrum with the Dot method is more as expected. It is continuous, which is as expected, but it is also negative in some parts, it appears to be offset in the negative y-axis. However, the amplitude of the spectrum did not represent the FFT amplitude, or the amplitude of the normalized signal. The amplitude was strongly related to modulation duty-cycle. It would be more convenient, if we could present a more stable amplitude independent of duty-cycle, perhaps, by the amplitude of the normalized signal. Hence, we took a different approach which processes the data per cycle.

### II. Method B: segment wise analysis

As the name implies, this method processes the data per segment. Figure 17 illustrates some aspects of this method. First, we smoothen the data by small amount to reduce the noise from signals. Second, we slice each signal into multiple segments, where each segment contains the modulation at the center. This can be done because we have knowledge of the modulation signal. Third, we discard all incomplete segments; these are usually the first and last frames. Fourth, we normalize each segment as earlier described, and finally, we remove the linear trends. While removing the linear trends, we noticed that the function (used by Matlab 'detrend') resulted in a shift in y-direction, which we displaced back to the correct position. To, displace it back to the correct position, the mean was calculated for time instances were modulation was off, and then subtracted from the segment. Next, we calculated the median over all segments, and read the value at instant of modulation end.

The final result is then the normalized amplitude of the signal. In Figure 17, on left is the median of signal segments for wavelength 577 nanometers, and on the right is the expected ePPG spectrum.

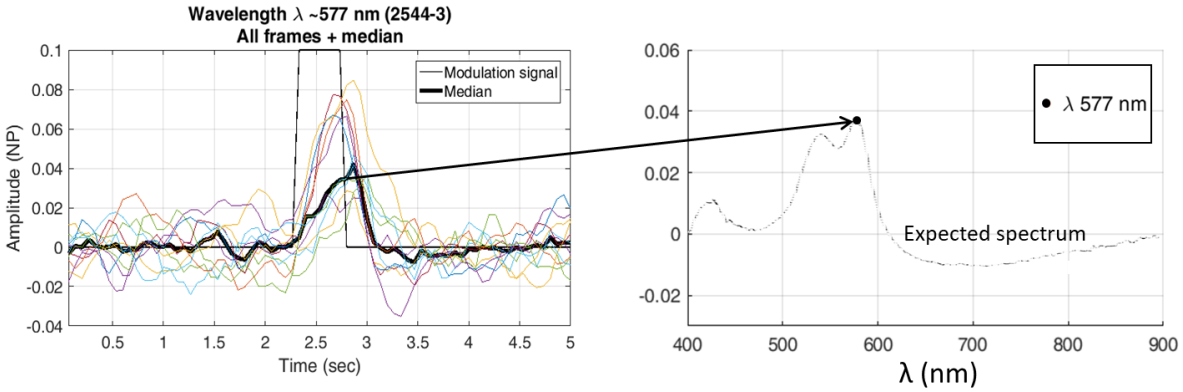


**Figure 17, On left the median of signal segments for wavelength 577nm, and on the right the expected ePPG spectrum**

While analyzing the resulted segments, we found that the signals with positive amplitude continue to increase for a short time (one frame '0.067 ms'), even after the modulation was off. This can be seen also in Figure 17 (left). This occurs due to the geometric effect: as soon as the air jet ends, the skin moves back because it is elastic, and as a result the optical effect (the reduced intensity) from the indentation disappears, resulting in an instantaneous increased intensity. The effect of the blood being removed is still present, it takes longer for the blood to flow back than that it takes for the indentation to disappear. For weak signals this effect was difficult to capture. To analyze the results in more illustrative manner, we plotted the median of signal segments in three dimensional space (wavelength, amplitude and time). This will allow us to visualize the change in spectrum over time (per median segment). In Figure 18, on the left is the resulted ePPG spectrum plotted vs FFT analysis, and on the right plotted in three dimensions. The frequency of modulation was set to 0.2 hertz, duty-cycle to 10% (half second) and the pressure to 16 mmHg (millimeters of mercury); it was measured from the Thenar eminence.

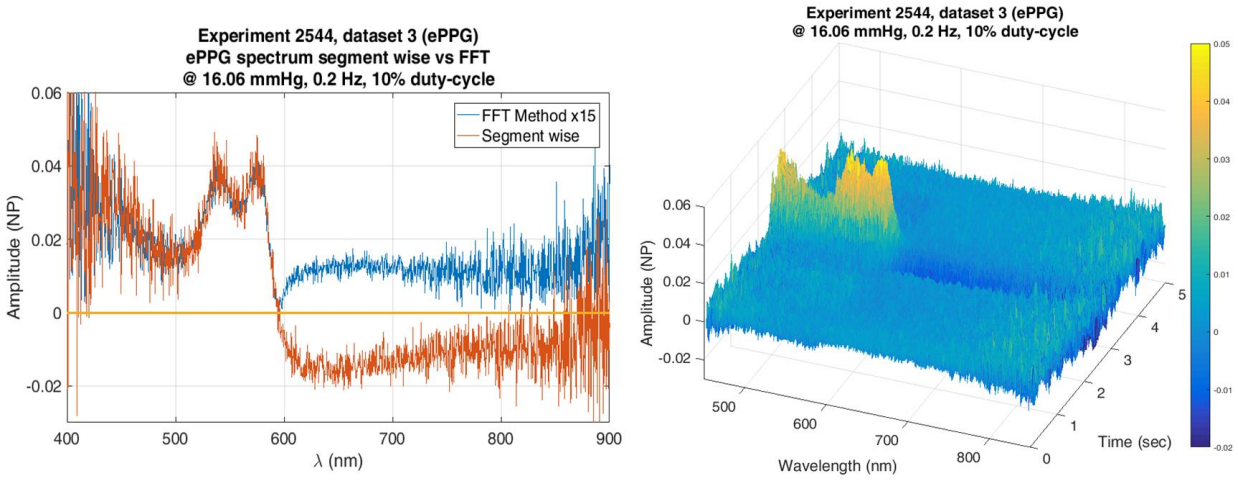


**Figure 18, on left the resulted ePPG spectrum plotted vs FFT, and on the right plotted in three dimensions**

Furthermore, to evaluate the results obtained by this method, we measured both the cardiac and external PPG. It was taken from the Thenar eminence, where the cardiac PPG is relatively strong and is thus easier to measure. Both measurements were taken from same skin area. To increase the signal to

noise ratio, the distance between the sensor and skin was reduced to 10 millimeters. Please note that the distance was reduced for the cardiac measurement only, the ePPG measurement was taken from 20 millimeters distance, both measurements were then analyzed. The external PPG was analyzed by the segment-wise method and the cPPG by the FFT analysis. To ensure correct cardiac PPG analysis, we used the frequency information obtained from the contact pulse-sensor. We then aligned both spectra to compare blood oxygenation difference. We found small deviations, but due to the high noise it was not enough to indicate the exact difference in blood oxygenation, thus, we can conclude that the ePPG was feasible. In Figure 19, the aligned spectra are plotted.

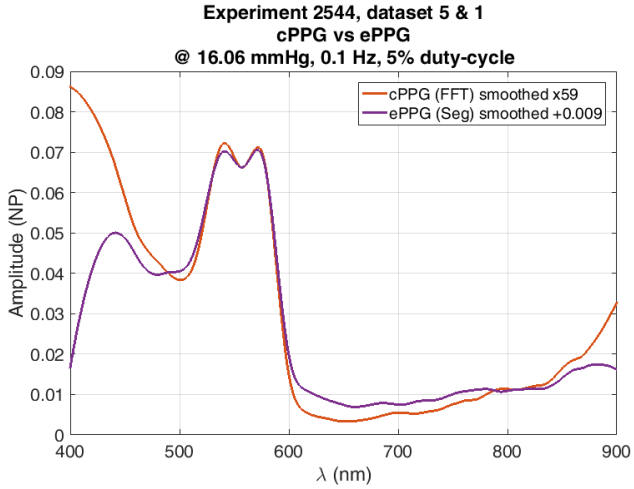


**Figure 19, ePPG vs cPPG spectra aligned for blood oxygenation comparison**

## Results

We characterized the air jet pressure in a quantitative way with two methods: the lateral scan and the differential method. Results showed that the differential method was accurate to estimate the pressure around the center. Using the lateral scan method, we measured only average pressure. Results obtained from pressure experiments using the differential method (Method B) showed that the pressure for nozzle diameter 2.5 millimeters at skin distance of 20 millimeters has comparable range to capillary blood pressure (Figure 10). Using shorter distances, higher pressure can be achieved; however the regulation of air flow becomes critical. Furthermore, results showed that the pressure was proportional to air flowrate squared. Please note that this relation was verified only in the range of our measurements. Then, we measured different skin sites and constructed the external PPG spectrum. We identified the geometric effect which was induced by the modulation. Consequently, the pressure and light intensity were reduced. The pressure change at the skin surface caused by the geometric effect was small, estimated to be less than 9%. Meanwhile, the change in light intensity was reduced by 24%. Actual measurements suggest an even stronger effect due to the geometry of used light beam. For this reason, we introduced two analysis methods which evaluate results for positive and negative amplitude. Both methods were evaluated and compared with the FFT analysis. The segment wise analysis was more preferable since it was capable to report stable and suitable amplitudes. We strongly recommend this analysis method for future work. Despite the geometric effect, the external PPG spectrum was constructed, and results have shown small deviations in spectrum compared to cardiac PPG spectrum. Results were as expected, some differences in blood oxygenation were found. Furthermore, we found

some interference between cPPG and ePPG for signals measured from Thenar eminence, which this may restrict the application of ePPG measurement to only weak cPPG sites. In total, 118 ePPG measurements were conducted. Most of the measurements were affected by the geometry change of skin. However, some locations had minimum change in geometry. For example, measurement (2482-4) was measured from skin site backed up by one of the metacarpal bones, which resulted in minimal skin geometric change. Result from (2482-4) showed that the ePPG is feasible if the geometric effect was minimized or eliminated. Also, the result showed potential solution for analysis of capillary refill time.

## Discussion

The current study showed that the external PPG by external pressure on human skin is feasible. In the presented method, we evaluated ePPG results using the shape of the resulting spectrum. However, to measure the exact oxygenation, we must compensate for the signal changes due to the geometric effect. The geometric effect is equal for all wavelengths, however, the amount of gain strongly depends on the change of skin geometry and light beam, and this is not a trivial problem. Therefore, we suggest studying this issue in future work, this may lead to skin elasticity or firmness measurement.

One possible solution is to minimize intensity drop using light reflector so that light is reflected from all directions to keep light intensity equal even when the skin geometry is changed. Other possible solution is to use a protocol to measure the geometric effect first, and then compensate the relative change. To measure the geometric effect, we can assume that the change in blood is slower than the geometry change of skin. Using this assumption we may disentangle the change in light intensity between blood and skin geometry. At the start of the modulation the change is rapid for both effects. After a while, change in blood is saturated and further change becomes negligible, and when the pressure is released, this will results in intensity increase as the geometry change of skin is faster than blood. This will result in signal increase which can be analyzed to produce the intensity increase due to the geometric effect (see small peak after air jet is off in Figure 17). Since signal at wavelength 577 nanometers has strong amplitude, we suggest using this protocol at comparable wavelength. Please note using the ratio of ratios method without compensating the geometric effect, oxygenation results will be incorrect.

Furthermore, to estimate the change in blood oxygenation between the cardiac and external PPG's, we compared both the ePPG and cPPG spectra. We anticipated that the ePPG would show lower oxygenation. Although some results appeared to show oxygenation differences (see bump between 700-800nm in Figure 19), the results were too noisy. The noise was one of the limiting factors to evaluate the oxygenation. Beside the noise and the geometric effect, the alignment of the sensor and air nozzle was very critical. A number of measurements were measured off center which led to even more geometric effect. Using camera sensor, such issues can be eliminated. However, the number of channels is less, which may hinder proper analysis. At this stage we suggest to continue using the spectrometer. With it, we can explore a wide range of wavelengths to target which wavelengths have the most reproducible results for ePPG. To solve alignment problems, we may consider using an optical lens splitter to split the optical image into two outputs, one can be used for the spectrometer and one for a camera. This will allow us to visualize the exact measured area while the spectrometer is in action. The company 'invisiblevision' markets the optical lens splitter which comes in two variants, 50/50 and 33/66. We suggest using the 33/66 since the spectrometer needs stronger light intensities. Then, to compensate light reduction caused by the splitter, we may consider decreasing the distance to skin.

Nevertheless, the reduction in light intensity by 1/3 may leave enough amount of light for ePPG measurement without decreasing the distance. However, there will still be one major drawback, which is the size of the splitter. This unit is very big, and we assume it is heavy as well, which may produce some noise from vibration. Furthermore, spectrometer noise in channels can be reduced by averaging channels. Results showed significant improvement when the number of channels was averaged to 256 channels. This will also reduce analysis time by factor of 8, but reducing spectrum channels must be done in a proper way. We initially assumed a linear distribution for channels, but this was incorrect, as the distribution of channels is non-linear. Please note that the distribution of channels tends to change with temperature.

In addition, it is worth noting that the external PPG is the opposite of the cardiac PPG signals. When the air pressure is applied, it will reduce the blood volume, while the cardiac PPG result in increase in blood volume. However, this does not violate the terminology of PPG (a volumetric measurement of an organ).

Due to time constraints, we did not investigate the effect of temperature, modulation frequency and duration (duty-cycle) on ePPG in sufficient depth. So far, we did not find significant change in ePPG spectrum while changing modulation frequency and duration. We suggest studying this parameter in future work.

In summary, we can conclude that contactless ePPG is feasible; we have clearly induced blood volume changes with the air jets. However, the geometric effect is a barrier for accurate measurement. The next step is to minimize or eliminate geometric effect, by the earlier suggested solutions, or by using smart algorithms to compensate for the change in intensity.

Whether the contactless ePPG may be used to quantify StO2 is considerably more challenging but demonstrating contactless ePPG in a reproducible and reasonably quantitative manner is a good first step.

## Conclusion

Most notably, up to our knowledge, this is the first study which investigated the effectiveness of contactless micro modulations to measure oxygen saturation in tissue. Our results provide a first step for feasible remote StO2 measurement. However, limitations such as the change in skin geometry and sensor noise are still limiting factors. Further improvements are needed to improve results and estimate the geometric effect accurately. Finally, finding the correlation between change in blood volume and the geometric effect may lead to measurement of skin elasticity or firmness.

## References


1. Ince, C. (2005). The microcirculation is the motor of sepsis. Critical Care, 9(Suppl 4), S13–S19. doi:10.1186/cc3753

2. Ince, C., and Sinaasappel, M. (1999). Microcirculatory oxygenation and shunting in sepsis and shock. Critical Care Medicine,27(7), 1369-1377. doi:10.1097/00003246-199907000-00031

3. D. E. Myers and J. C. Jones. (May 19, 2009). Dynamic StO2 measurements and analysis. U.S. Patent No. US 7,536,214 B2. Washington, DC: U.S. Patent and Trademark Office. Hutchinson Technology Incorporated, Hutchinson, MN (US)

4. Verkruysse, W., Svaasand, L. O., and Nelson, J. S. (2008). Remote plethysmographic imaging using ambient light. Optics Express,16(26), 21434. doi:10.1364/oe.16.021434

5. M. Poh, D. McDuff, and R. Picard, (2010). Non-contact, automated cardiac pulse measurements using video imaging and blind source separation. Opt. Express 18, 10762-10774

6. Guazzi, A., Villarroel, M., Jorge, J., Daly, J., Frise, M., Robbins, P. and Tarassenko, L. (2015). Non-contact measurement of oxygen saturation with an RGB camera. Biomedical Optics Express, 6(9), p.3320.

7. van Gastel, M., Stuijk, S. and de Haan, G. (2016). New principle for measuring arterial blood oxygenation, enabling motion-robust remote monitoring. Scientific Reports, 6(1).

8. Verkruysse, W., Bartula, M., Bresch, E., Rocque, M., Meftah, M., and Kirenko, I. (2017). Calibration of Contactless Pulse Oximetry. Anesthesia & Analgesia,124(1), 136-145. doi:10.1213/ane.0000000000001381

9. Oak, S., Aroul, P. (2015). How to Design Peripheral Oxygen Saturation (SpO2) and Optical Heart Rate Monitoring (OHRM) Systems Using the AFE4403 (Application Report No. SLAA655). Retrieved from Texas Instruments website: http://www.ti.com/lit/an/slaa655/slaa655.pdf

10. Gioux S., Mazhar A, Lee BT, Lin SJ, Tobias AM, Cuccia DJ and Stockdate A. (2011). First-in-human pilot study of a spatial frequency domain oxygenation imaging system. J. Biomed. Opt. 0001;16(8):086015-086015-10. doi:10.1117/1.3614566.

11. Verkruysse, W., Zhang, R., Choi, B., Lucassen, G., Svaasand, L. O., and Nelson, J. S. (2004). A library based fitting method for visual reflectance spectroscopy of human skin. Physics in Medicine and Biology,50(1), 57-70. doi:10.1088/0031-9155/50/1/005

12. De Haan, G. D., and Leest, A. V. (2014). Improved motion robustness of remote-PPG by using the blood volume pulse signature. Physiological Measurement,35(9), 1913-1926. doi:10.1088/0967-3334/35/9/1913

# Appendix

## General information

**Aligning the spectrometer:**

To align the microprobe-lens and nozzle to single point, the camera 'UI-3060CP-C-HQ' is used. Due to space limitations, the angle between both units was approximately 20˚.

1. Placed area of skin (hand) at a distance of 20mm
2. Then align air indentation to image center.
3. Using a ring spacer, cover the image with only area of air pressure.
4. Adjust the focus using the microprobe-lens focus wheel.
5. Finally, to ensure scenario as in pressure experiments (air was perpendicular to probe/skin), maximize the angle to most vertical to skin for both units (the lens and nozzle).

**Warnings:**

- **Please, make sure to first connect the air control unit to the PC (via USB) before connecting it to the net power**. Connecting the air control unit in different sequence may cause to failure results. This is important, since the microcontroller initialize the serial communication only at the start.
- **Please do not exceed the maximum ratings for light source**. The maximum rating is 24volts for 250watt. It means maximally it can be set to 24 volts and 10.4 ampere; we set it to ~190watt (19.8volts and 9.4 ampere) due to heat issues. This will also ensure longer lamp usage (longer age).
- **Please do not take measurement longer than 10 minutes**. Please, always give some rest to cool down the light source unit. The halogen lamp used is very powerful, which temperature can reach up to 500 C˚. Using the lamp for long periods will cause heat issues.
- **Please do not exceed the maximum ratings for air control unit**. The maximum rating is 12volts and at least 500mA (milliamps).
- **Poor peripheral perfusion and motion may cause bad results for the PPG contact sensor.** Please always choose the optimal site for probe placement. So far, the ring finger with the LED facing skin from the inner side of the hand (LED is the opposite to nail side) showed good results, but feel free to choose your favorite location.

**Kwon issues:**

1. (Only for spectrometer) Lowering the resolution of channels will result in incorrect channel distribution. We suggest using the full resolution (2048 channels), else before use please consider fixing this problem. While development we assumed linear distribution between channels, this assumption was incorrect. The distribution of channels is non-linear. In addition, distribution of channels tends to change upon temperature change.
2. The distance sensor fails to measure the distance while the light source is 'On'. The light source is powerful such that signal from the sensor is distort.
3. The Air control unit must be first connected to PC (via USB), then to the net power (power adapter), or else failure operation may result. This issue can be solved by allowing the microcontroller to wait during the initialization routine for connection before starting with general routine.
4. While measuring, if the software was terminated using termination button (the red dot in LabView), the information file then is incomplete. This is because information file is written at the end of the measurement. This is because some information such as duration cannot be calculated in advance. So, please always use 'Stop' button to terminate the software, this will ensure correct software operation. The 'Stop' button has a keyboard short key; it is the 'ESC'.
5. The frequency measured from the contact pulse sensor contains also modulation frequency. This issue is caused by the rapid change in power when the solenoid value is on. The voltage regulation unit is slow to compensate the change in power, which effect the ADC measurement. To solve this issue, we suggest measuring the contact pulse sensor with the distance senor using the second unit (the distance unit), this is the easiest and cheapest solution.

**Troubleshooting:**

1. Very noisy PPG signal from contact senor. Please check LED position (use inner location of the finger), choose different finger for better signal and minimize motion. Please see figure from software chapter.
2. 'Labview' runs slow.
    a. Check the RS-232 connections (serial com-port). Failure connection may cause a read time out, which may slow system.
    b. Check system applications running on the background, such as Windows Updates or Antivirus.
    c. Check analysis window size. Increasing window size results in increasing CPU resource.
3. 'Labview' start, but it shows errors when running.
    a. Check LabView Vision license.
    b. Check Ocean Optics SDK software, this must be installed and linked to LabView VI's.

**List of components used by both setups:**

Pressure setup:

- Scale - model: PB1502-S/FACT
- Distance sensor (1) - model: ST-VL6180X
- Distance sensor (2) – model: ST-VL53l0X
- Air flow meter – range 1 to 25 L/min
- PC – Window 7 Enterprise 64-bit operating system
- Micro-controller – ATmega328
- Software – LabView 2014 SP1 32-bit

ePPG setup:

- Remote PPG sensor – Ocean Optics USB2000
- Microprobe-lens - model: Volpi AS 14/50
- Contact pulse-sensor - model: SEN-11574
- Distance sensor - model: ST-VL6180X
- PC – Window 7 Enterprise 64-bit operating system
- Software – LabView 2014 SP1 32-bit
- Micro-controller x2 – ATmega328 ()
- DC laboratory power supply - model: SM7020-D
- Halogen lamp – Osram GX5.3 24V/250W
- Camera (for alignment) – model: UI-3060CP-C-HQ

## Software (LabView)

In order to acquire ePPG signals, we have developed a tool using the software 'LabView 2014 SP1 32-bit'. Below a short description on how to start and use this tool to acquire ePPG signals.

- Start the PC and make sure it has booted completely.
- Before starting the VI (the software in 'LabView'), please make sure the following steps are taken in the right order,

    1. Make sure the power supply of the air control unit is unplugged from the net supply. **This step is very important**. However, it is required only when the PC was rebooted, or the USB port was unplugged.
    2. Connect the air control unit and the spectrometer to the PC via the USB port. See figure below,

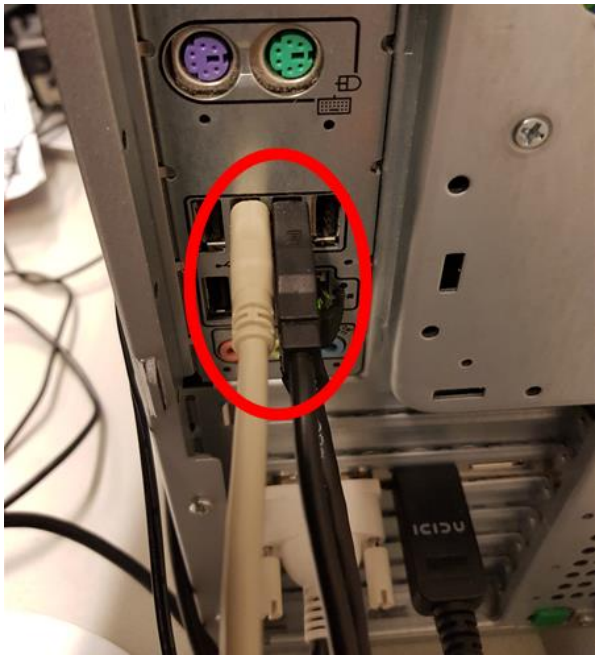

    3. Check the LED of the air control unit. It should blink between white and blue. If not, please check the USB cable.

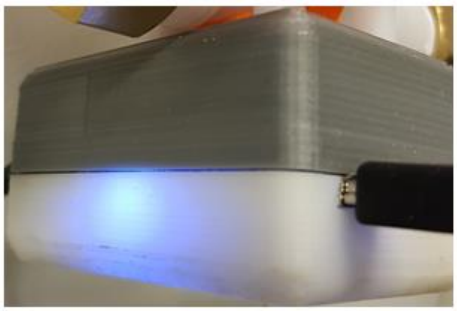
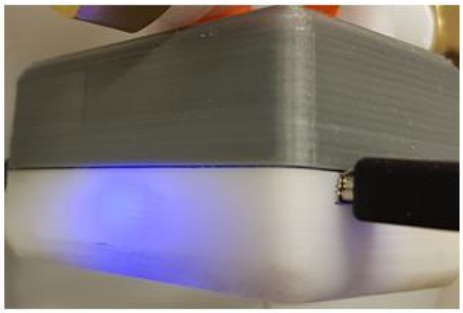

4. On Windows navigate to Device Manager. This can be done in various ways. If you are not familiar with, please follow the following steps, click ‘Start’ (1), then right-click on ‘Computer’ (2), then click on ‘Properties’ (3). See figure below,

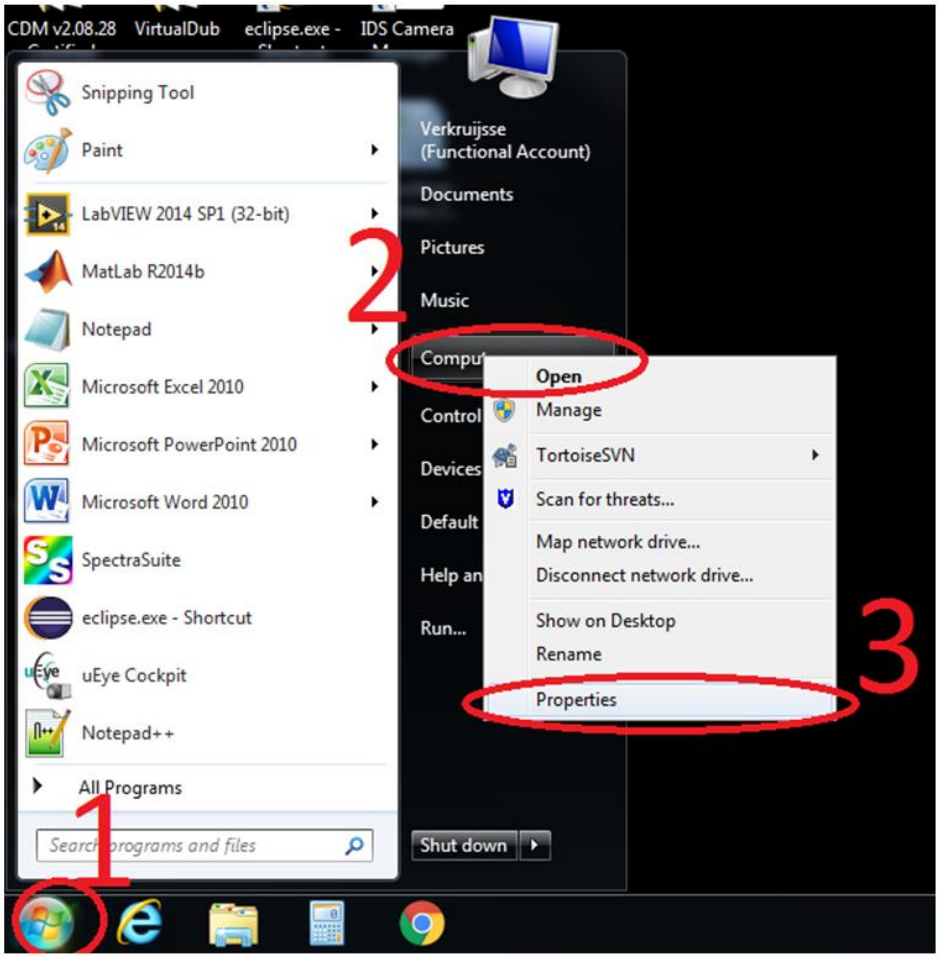

5. Click ‘Device Manager’.

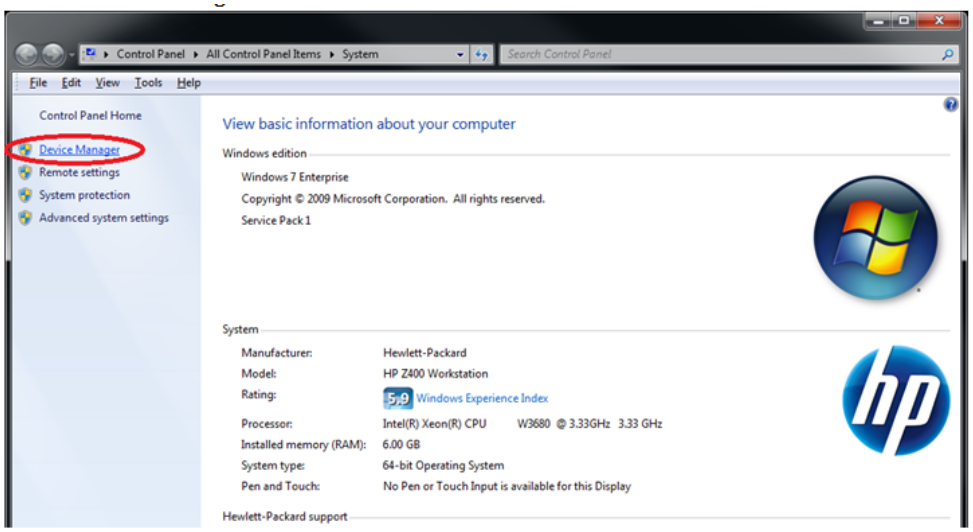


6. You should get following screen, please click on ‘Ports (COM & LPT)’, and then note the allocated COM port (in this case it is COM3). If you cannot find any the port, it means the drivers are not installed yet, or the cable/USB port is defect, or else the hardware is defect. If the port is presented please skip step 7.

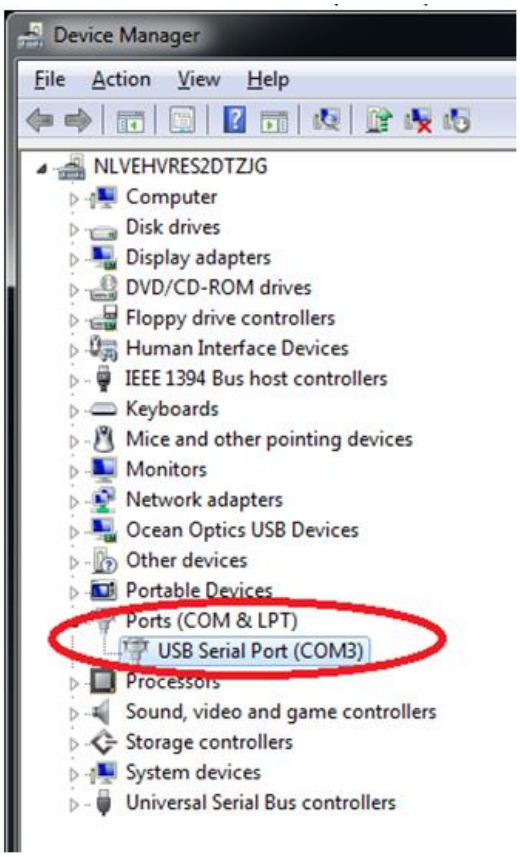

7. To install the driver, please install **FTDI** driver version **2.8.28.0**. This is the only working version. To check the driver is correctly installed, follow instruction from 4 to 6, and then double click on the 'USB Serial Port' icon. You can check 'Device status' field.

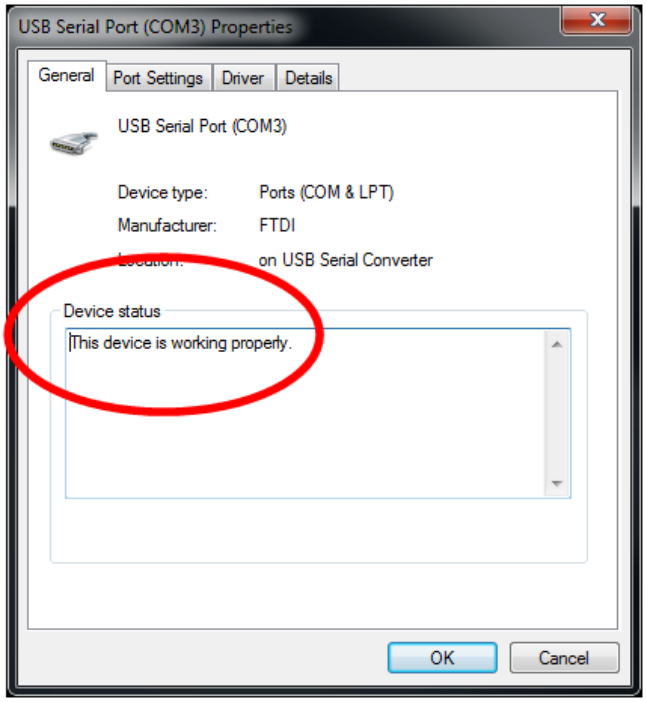


To check the version of the installed driver, click on 'Driver' tab (1), and then check the 'Driver Version' (2). Then, close by clicking 'OK' bottom (3).

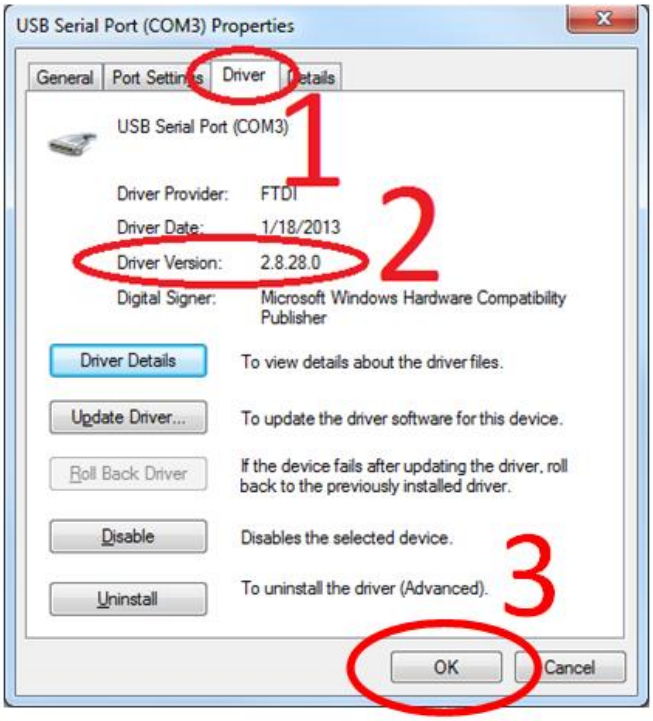

8. Connect the second micro-controller (the distance unit) via the USB to the PC. Then, note the second COM port appeared after connecting the second micro-controller (in this case it is COM9). Please see figure below,

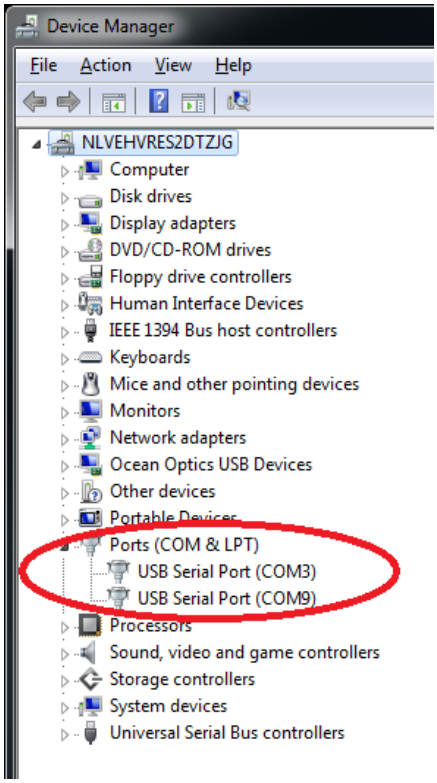


- Now we have identified both COM Ports. We may configure 'LabView' VI. Start 'LabView' VI by navigating to folder 'StO2-code' (1), and then choose the most recent version (2).

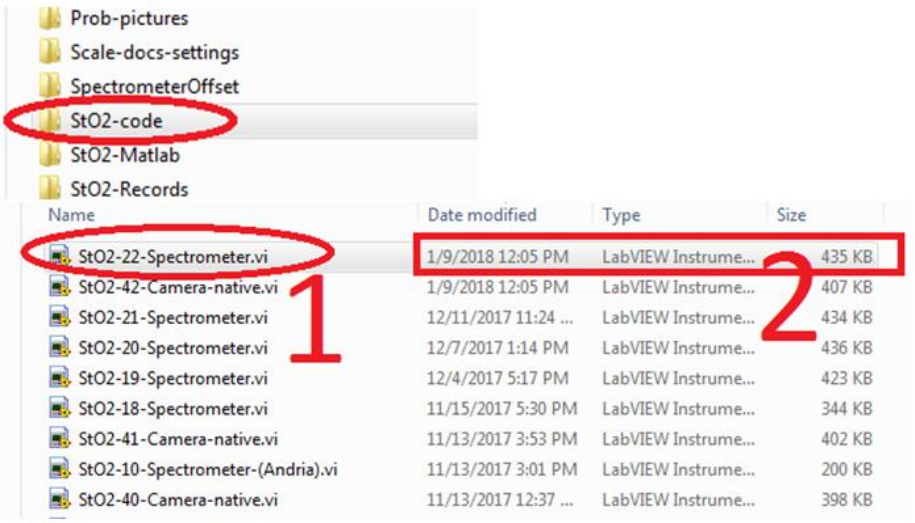

- Select the correct port for each unit (squared in red).

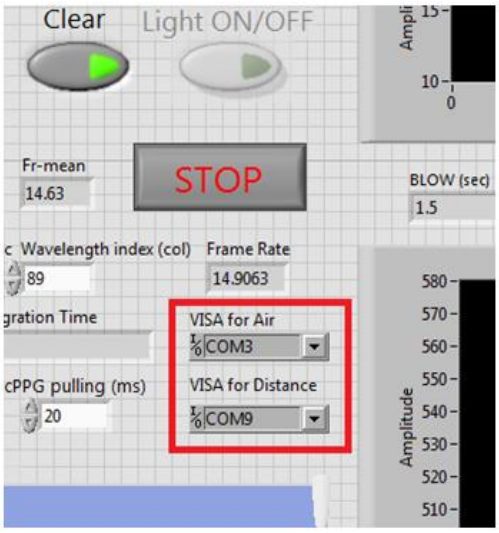


- Connect the air control unit to power supply.

- Switch the Laboratory power supply (1), and then set to the desired output (2). We suggest setting it to 20 volts and 10.5 ampere.

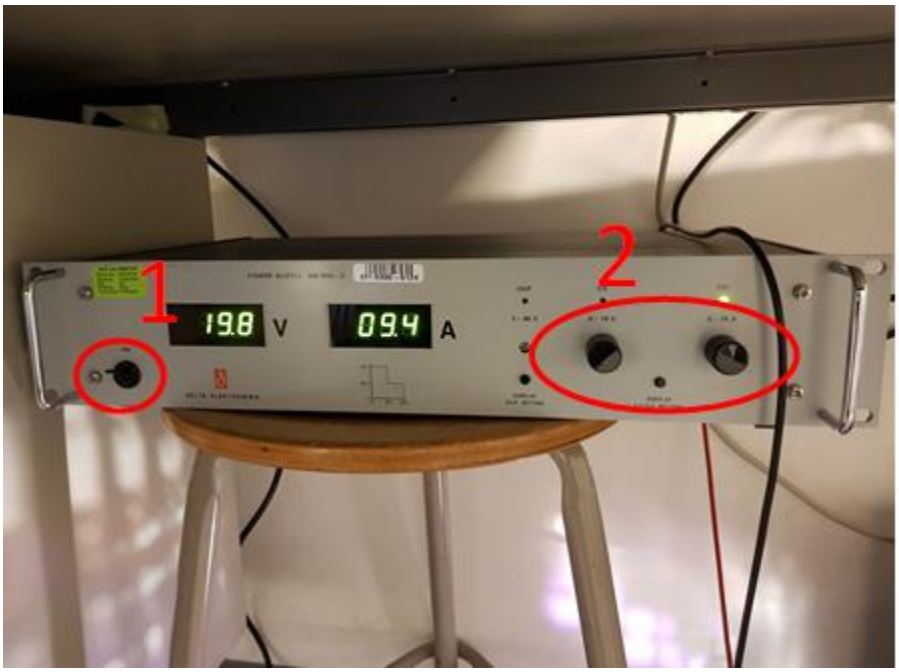


- Open the faucet of air chamber.

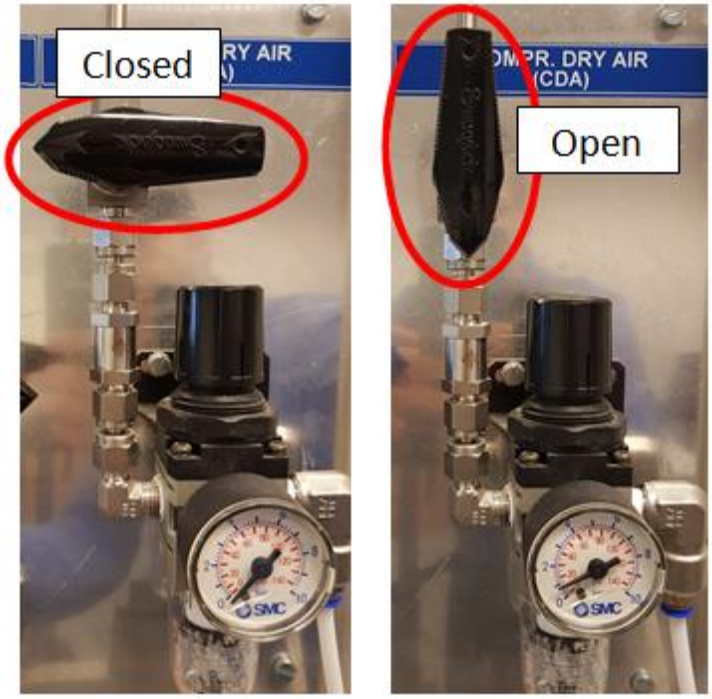

- Check the valve is functioning. Using the bottom circled in red, it should trigger air valve manually.

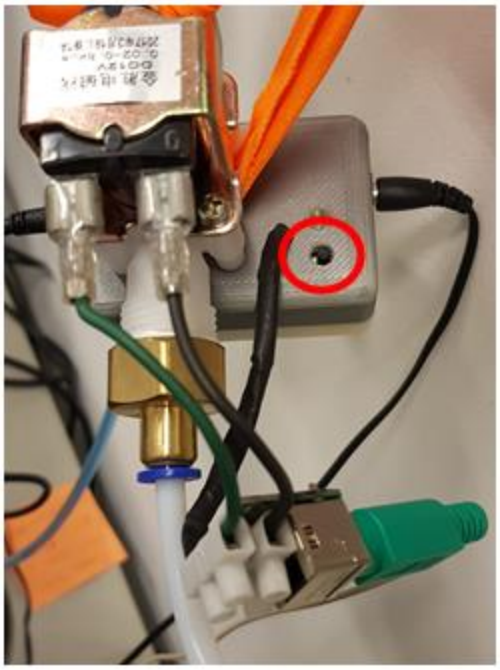

- Wear the contact PPG sensor as shown in figure. You may choose a different finger, but LED side must be attached accordingly.

- In ‘LabView’ VI, check the file paths whether these are set correctly (1). The 1st path is to locate results path. The 2nd path is to locate the file which presents the pattern of modulation. This file has specific structure so please be careful while modifying (be careful with ‘Enters’ and ‘Spaces’). The 3rd path is to locate the configuration file; this file contains only the numbering of experiments.

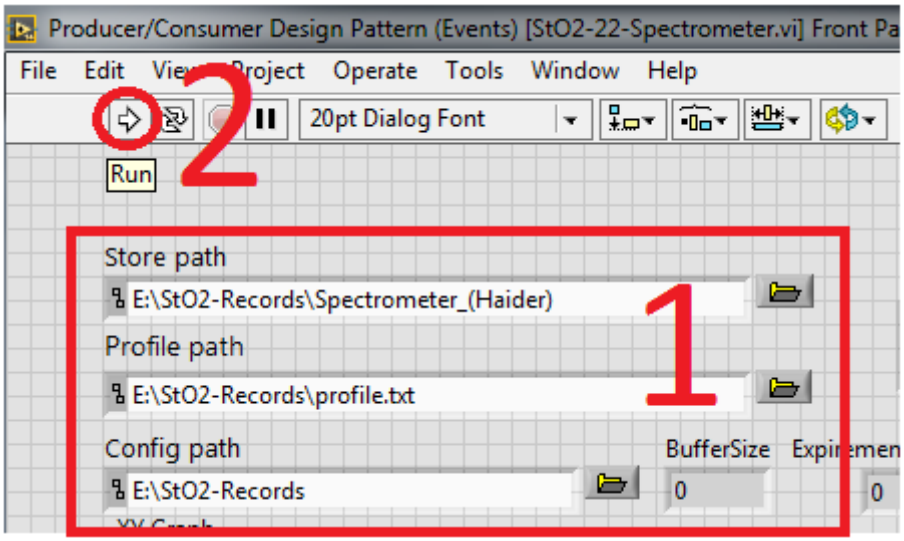


Below, an example for files, the ‘config.txt’ and ‘profile.txt’. Please note that both files must be kept with the same naming. The file ‘profile.txt’ is per line structured as measurement duration, frequency of modulation, modulation duty-cycle and light state (1=On, 0=Off). For proper processing of data (in ‘Matlab’) and cooling down the light source, we suggest you to use short pauses between measurements. This can be done using the line ‘5,0,0,0’, which result in rest for the light unit for 5 seconds. This should be sufficient to cool down the unit, especially when measurement durations are less than 4 seconds per line. For longer periods we suggest to take 10 to 15 seconds of rest.

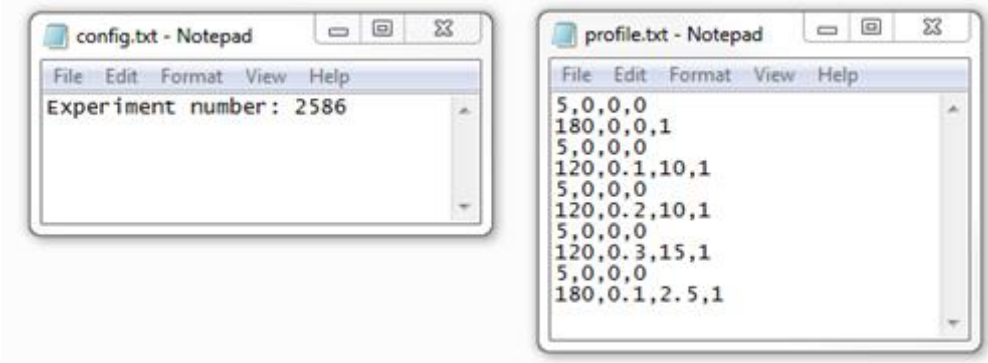


Then you can start ‘LabView’ by clicking on ‘run’ bottom (2).

- To start measuring, two modes can be used, the ‘Profiled’ and the ‘Fixed’.

    1. The ‘Fixed’ mode measures at a fixed frequency and duty-cycle. To measure, set the parameters in (1), the ‘Air frequency’ and ‘Air duty-cycle’ to the desired value, then switch the mode to ‘Fixed’ (2) dark green (off) means fixed mode is selected, then click ‘Record ON/OFF’ (3). When you wish to stop recording, click ‘Record ON/OFF’ again to stop. If you wish, you can register all information of measurement to text file; you can fill fields in (4). Although, we always encourage you to fill these fields, it is very nice way of bookkeeping the information of the data/records.

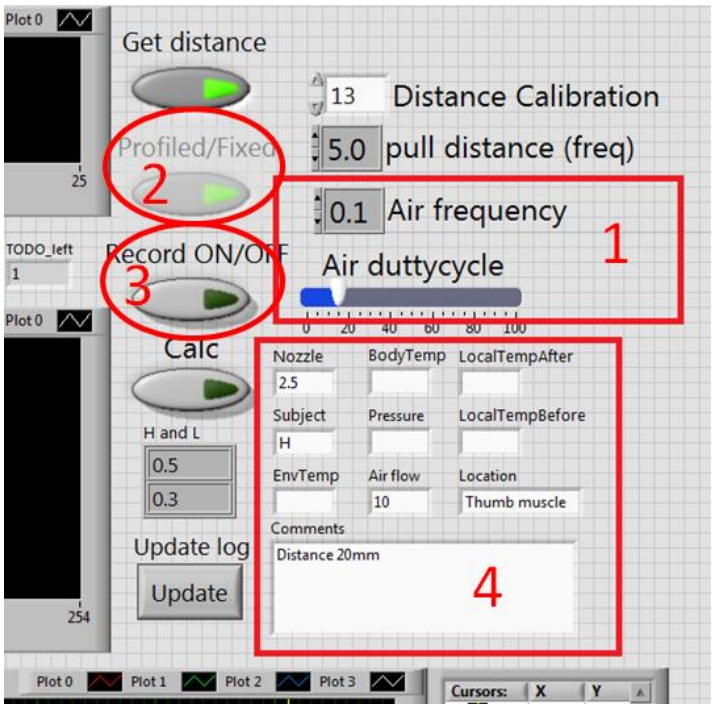


    2. The ‘Profiled’ mode measures multiple sequences. It adapts the frequency and duty-cycle by the given profile in file (profile.txt). To start, set to profiled mode using (2) green means profiled mode is selected. Then, click ‘Record ON/OFF’ (3), when the pre-defined sequence (the profile) finish, if will stop automatically. Here as well, we encourage you to fill information fields in (4).

- At the end, when the measurement is finished, the software will generate two files. One is the information file (yyyy_@xxxx.txt) where the ‘yyyy’ is the date and ‘xxxx’ is the number of the experiment, which the can be seen below,

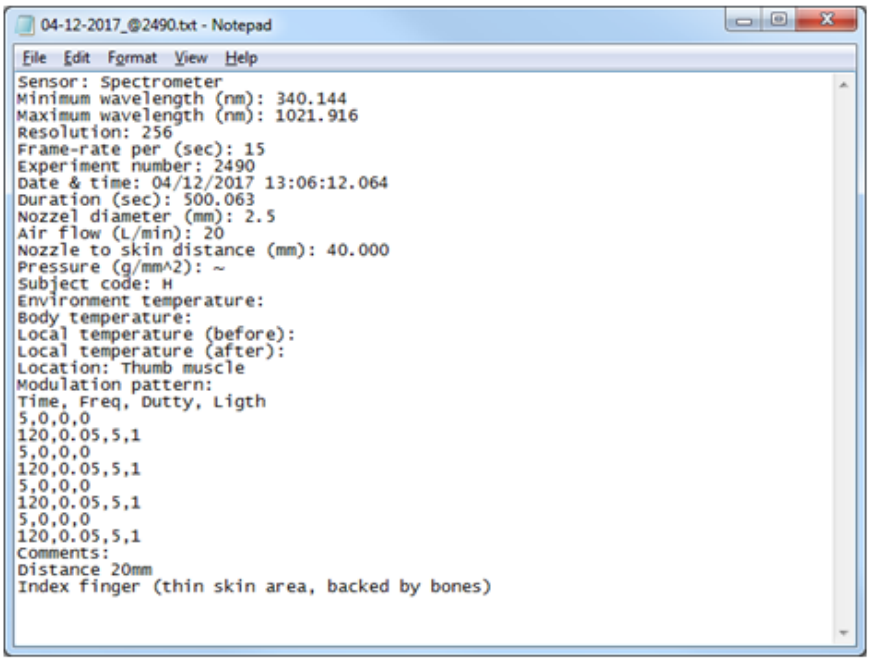


The second file (SpectData@xxxx.csv) contains the data of signals. The 'xxxx' refers to the number of experiment. Please note that the first line contains the information of the distribution of wavelengths. Also, note that the first channel of the spectrometer is always 0, we do not know why, perhaps, it is a bug from Ocean Optics. To read the data, you can consider it as a table, each line contains a sample of all measurements. Column-wise, it starts by spectrometer channels, then the measurement values of the contact PPG sensor, time and finally the state of the light source (1=On, 0=Off). Below, an example of such file showing the last columns of the data file.

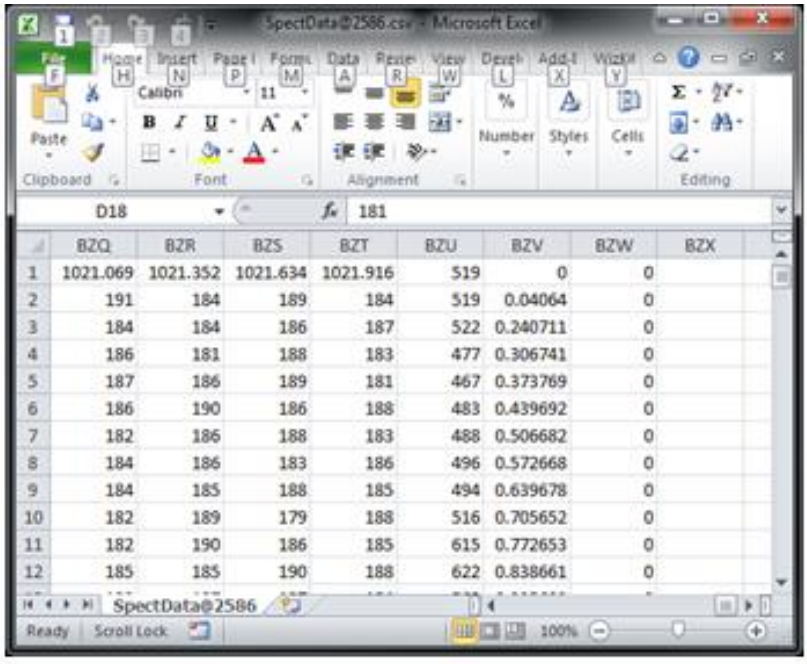

## Firmware 1: (Air control unit)

To test commands, you can use any serial monitoring software, we used Arduino serial monitor. Please note sensor values are sent with ending line.

```
/*
 * Serial events can be interpreted as:
 * ------------------------------------
 * code   | Function
 * ------------------------------------
 * t      | Short beep twice
 * b      | Short beep once
 * B      | Long beep ocne
 * 0      | Turn valve off
 * 1      | Turn valve on
 * c or C | Update color (color sould be in hex: ex FFFFFF => white)
*/

//#include <avr/wdt.h>
#include <NeoPixelBus.h>
// LED_BUILTIN
#define totalLEDs      8
#define buzzerPin      4
#define redLedPin      5
#define greenLedPin    6
#define relayPin       7
#define buttonPin      8
#define PixelPin       9
#define PulseSensorPin 0 // Pulse Sensor PURPLE WIRE connected to ANALOG PIN 0
#define pulseInterval  66 // In milliseconds ~66.667 ms equal to camera framerate 15 per second
#define ledInterval   1000
#define buzzerShortInterval  50
#define buzzerLongInterval   200
#define firstBuzzerInterval  50
#define secondBuzzerInterval 100
#define thirdBuzzerInterval  150

int Signal;                // holds the incoming raw data. Signal value can range from 0-1024
byte red = 128;
byte green = 128;
byte blue = 128;
byte colorChannel = 0;
bool relayState = LOW;
bool redLedState = LOW;
bool greenLedState = LOW;
bool innerLedState = LOW;
bool updateColor = false;
bool longBuzzerState = LOW;
bool shortBuzzerState = LOW;
bool twoShortBuzzerState = LOW;
unsigned long previousMillisLong = 0;
unsigned long previousMillisShort = 0;
unsigned long buzzerMillis = 0;
const uint16_t PixelCount = totalLEDs;
NeoPixelBus<NeoGrbFeature, Neo800KbpsMethod> strip(PixelCount, PixelPin);

void setup() {
  // Opening the serial port
  Serial.begin(115200);

  // Initializing pins
  pinMode(LED_BUILTIN, OUTPUT);
  pinMode(buzzerPin, OUTPUT);
```

```
  pinMode(redLedPin, OUTPUT);
  pinMode(greenLedPin, OUTPUT);
  pinMode(relayPin, OUTPUT);
  pinMode(buttonPin, INPUT_PULLUP);

  digitalWrite(buzzerPin, LOW);
  digitalWrite(redLedPin, redLedState);
  digitalWrite(greenLedPin, greenLedState);
  digitalWrite(relayPin, relayState);

  // this resets all the neopixels to an off state
  strip.Begin();
  RgbColor newColor(red, green, blue);
  for(int i=0; i<totalLEDs; i++){
    strip.SetPixelColor(i, newColor);
  }
  strip.Show();

  //wdt_enable(WDTO_2S);
}

void loop() {
  unsigned long currentMillis = millis();

  if (currentMillis - previousMillisShort >= pulseInterval) {
    Signal = analogRead(PulseSensorPin);  // Read the PulseSensor's value.
    Serial.println(Signal);               // Send the Signal value to Serial Plotter.
    previousMillisShort = currentMillis;
  }

  if (currentMillis - previousMillisLong >= ledInterval) {
    // save the last time you blinked the LED
    previousMillisLong = currentMillis;
    innerLedState = !innerLedState;
    //greenLedState = !greenLedState;
    digitalWrite(LED_BUILTIN, innerLedState);
    //digitalWrite(greenLedPin, greenLedState);
  }

  if(!relayState){
    bool button = digitalRead(buttonPin);
    digitalWrite(relayPin, !button);
    digitalWrite(redLedPin, !button);
  }

  if(shortBuzzerState){
    if (currentMillis - buzzerMillis >= buzzerShortInterval){
      digitalWrite(buzzerPin, LOW);
      shortBuzzerState = LOW;
    }
  }

  if(longBuzzerState){
    if (currentMillis - buzzerMillis >= buzzerLongInterval){
      digitalWrite(buzzerPin, LOW);
      longBuzzerState = LOW;
    }
  }

  if(twoShortBuzzerState){
    if (currentMillis - buzzerMillis >= thirdBuzzerInterval){
      digitalWrite(buzzerPin, LOW);
      twoShortBuzzerState = LOW;
    }else if (currentMillis - buzzerMillis >= secondBuzzerInterval){
      digitalWrite(buzzerPin, HIGH);
    }else if (currentMillis - buzzerMillis >= firstBuzzerInterval){
```

```
      digitalWrite(buzzerPin, LOW);
    }
  }

  if(updateColor){
    if (Serial.available()>0){
      // Process the incoming Byte:
      if(colorChannel == 0){
        red = Serial.read();
        colorChannel++;
      }else if(colorChannel == 1){
        green = Serial.read();
        colorChannel++;
      }else{
        blue = Serial.read();
        RgbColor newColor(red, green, blue);
        for(int i=0; i<totalLEDs; i++){
          strip.SetPixelColor(i, newColor);
        }
        strip.Show();
        colorChannel = 0;
        updateColor = false;
      }
    }
  }

  //wdt_reset();
}

void serialEvent() {
  if(!updateColor){
    switch(Serial.read()){
      case 't':
          twoShortBuzzerState = HIGH;
          buzzerMillis = millis();
          digitalWrite(buzzerPin, twoShortBuzzerState);
        break;

      case 'b':
          shortBuzzerState = HIGH;
          buzzerMillis = millis();
          digitalWrite(buzzerPin, shortBuzzerState);
        break;

      case 'B':
          longBuzzerState = HIGH;
          buzzerMillis = millis();
          digitalWrite(buzzerPin, longBuzzerState);
        break;

      case '0':
          digitalWrite(relayPin, LOW);
          relayState = LOW;
        break;

      case '1':
          digitalWrite(relayPin, HIGH);
          digitalWrite(redLedPin, HIGH);
          relayState = HIGH;
        break;

      case 'c':
      case 'C':
          updateColor = true;
        break;
```

```
      case 0:
      case '\n':
          // Do nothing !! it is an string terminator
        break;

      default:
          digitalWrite(relayPin, LOW);
          relayState = LOW;
      break;
    }
  }
}
```

### Firmware 2: (Distance unit)

To test commands, you can use any serial monitoring software, we used Arduino serial monitor. Please note sensor values are sent with ending line.

```
/*
 * Serial events can be interpreted as:
 * -------------------------------------
 * code   | Function
 * -------------------------------------
 * d or D | Get distance
 * l      | Light/Laser Off
 * L      | Light/Laser On
 */

#include <Wire.h>
#include <VL6180X.h> // from kevin-pololu

#define LASER_PIN 7

// Valid scaling factors are 1, 2, or 3.
#define SCALING 1
VL6180X sensor;
bool  getDistance = false;

void setup()
{
  // Opening the serial port
  Serial.begin(115200);
  pinMode(LED_BUILTIN, OUTPUT);
  pinMode(LASER_PIN, OUTPUT);
  Wire.begin();

  sensor.init();
  sensor.configureDefault();
  sensor.setScaling(SCALING);

  // Extra, for continuous measurements
  sensor.writeReg(VL6180X::SYSRANGE__MAX_CONVERGENCE_TIME, 30);
  sensor.writeReg16Bit(VL6180X::SYSALS__INTEGRATION_PERIOD, 50);

  sensor.setTimeout(500);
  delay(300);
  // start interleaved continuous mode with period of 100 ms
  sensor.startInterleavedContinuous(100);

  digitalWrite(LED_BUILTIN, LOW);
  digitalWrite(LASER_PIN, LOW);
}

void loop() {
```

```
  if(getDistance){
    //int distance = sensor.readRangeSingleMillimeters();
    int distance = sensor.readRangeContinuousMillimeters();
    if(!sensor.timeoutOccurred()) Serial.println(distance);

    getDistance = LOW;
    digitalWrite(LED_BUILTIN, LOW);
  }
}

void serialEvent() {
    switch(Serial.read()){
      case 'd':
      case 'D':
          getDistance = HIGH;
          digitalWrite(LED_BUILTIN, HIGH);
        break;

      case 'l':
          digitalWrite(LASER_PIN, LOW);
          break;

      case 'L':
          digitalWrite(LASER_PIN, HIGH);
          break;

      case 0:
      case '\n':
      default:
          // Do nothing !! it is an string terminator
        break;
    }
}
```

## Data (resulted spectra for all measurements)

(Confidential information) please contact professor W. Verkruijsse for info.